GLUTEN COMPOSITES WITH FUNCTIONALLY MODIFIED CELLULOSE NANOFIBERS

Muhammad Usama Asghar

Registration No: 02272113018

Supervised by

Dr. Faiza Rasheed

Department of Biotechnology

Faculty of Biological Sciences

Quaid-I-Azam University

Islamabad, Pakistan 2023

Gluten Composites with Functionally Modified Cellulose Nanofibers

A thesis submitted in the partial fulfillment of the requirements for the degree of Master of Philosophy in biotechnology.

BY

Muhammad Usama Asghar

Department of Biotechnology

Faculty of Biological Science

Quaid-I-Azam University

Islamabad, Pakistan

2023

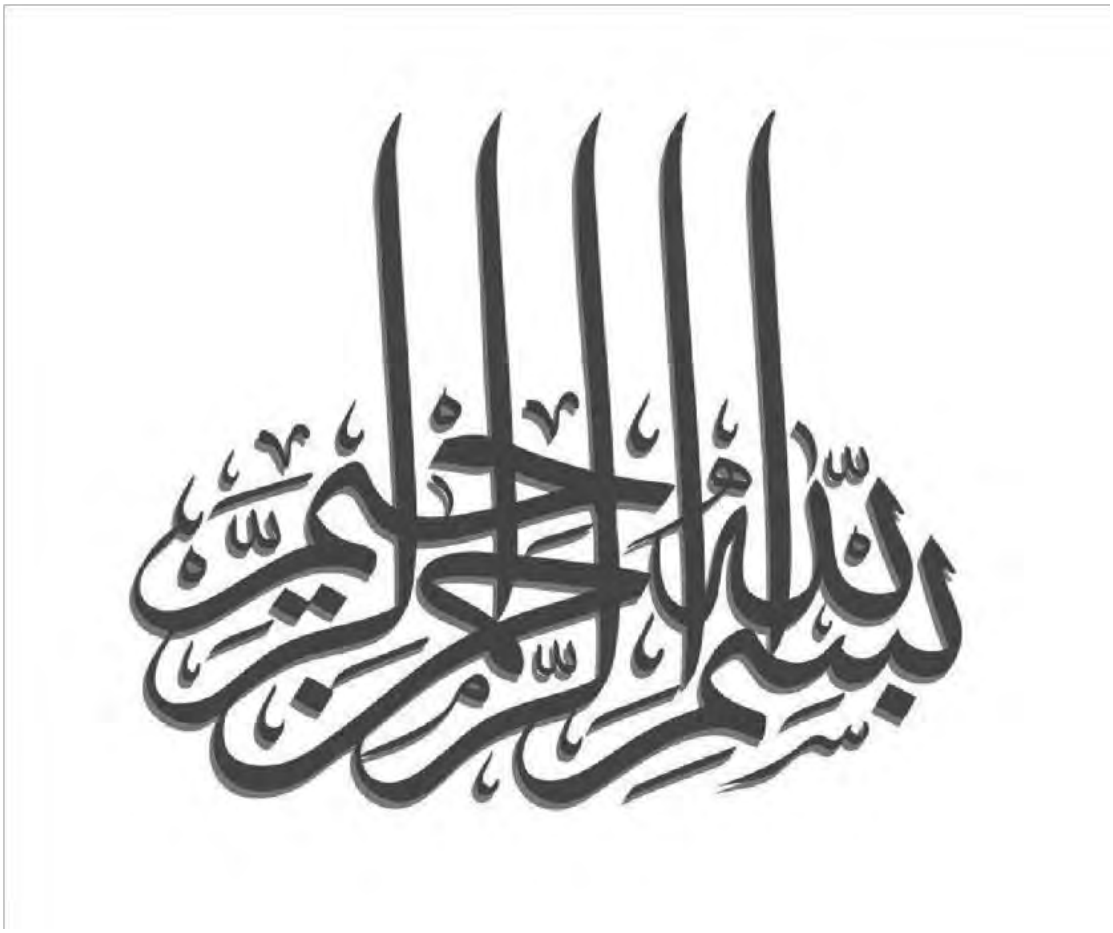

the name of Allah, The Most Gracious, The Most Merciful.

DECLARATION

I hereby affirm that the work provided in this thesis is entirely my own creation, except for any places where it has been acknowledged. Nothing from this thesis has ever been published or submitted for consideration for another degree or certificate.

Signature of student

Muhammad Usama Asghar

Registration No: **02272113018**

CERTIFICATE OF APPROVAL

This is to certify that the research work presented in this thesis, entitled **"Gluten composites with functionally modified cellulose nanofibers"** was conducted by **Mr. Muhammad Usama Asghar** under the supervision of **Dr. Faiza Rasheed.**

No part of this thesis has been submitted anywhere else for any degree. This thesis is submitted to the Department of Biotechnology, Faculty of Biological Sciences, Quaid-i-Azam University, Islamabad, Pakistan, in partial fulfillment of the requirements for the Degree of Master of Philosophy in the field of Biotechnology.

Supervisor _____

Dr. Faiza Rasheed

External Examiner _____

Dr. Tayyabba Yasmin

Chairperson _____

Dr. Javeria Qazi

Dated: 26/10/2023

DEDICATION

I dedicate my work to my supervisor **Dr Faiza Rasheed**, as well as to all my labmates and friends, who were very supportive and inspired me throughout the entire research work. Specifically, I dedicate this effort to my devoted and honorable parents who have always supported, encouraged, advised, and prayed for me.

Muhammad Usama Asghar

ACKNOWLEDGEMENTS

I am grateful to **ALLAH** Almighty, the Most Merciful and the Most Beneficent, Who gave us health and the capacity to learn about some of the numerous things that His creation offers, as well as the ability to carry out this research project successfully.

I am appreciative of my kind supervisor, **Dr. Faiza Rasheed**, for her personal interest, insightful advice, constructive criticism, encouragement, and ongoing support throughout the entirety of my research project. Her helpful demeanor, practical knowledge, and patronizing concern gave me access to the center's facilities in a proper, suitable, and beneficial way. I'm also appreciative to our chairperson, associate professor **Dr. Javeria Qazi**, for supporting me during my studies and being so kind to me.

I want to thank my lab mates Muhammad Razeen Ahmad, Hifsa Abbasi, Sanam Gull Arshad, Aiman Areej, Ayesha Maqsood, Suleman Khan, Bilal Saeed and Nageena Arif for their insightful advice and helpful suggestions during my lab experiments. I want to sincerely thank all my dear friends Misbah Zeb Kiani, Muhammad Mustajab khan, Bushra Khan, Hassan Ayaz, and Ukasha Khalid for their attention, unceasing encouragement, friendly advice, and continuous support during my study.

Muhammad Usama Asghar

Table of Contents

LIST OF TABLES

LIST OF FIGURES

LIST OF ABBREVIATIONS

AGE	Allyl Glycidyl Ether
AGU	Anhydrous Glucose Units
BCNCs	Bacterial Cellulose Nanocrystals
BCNFs	Bacterial Cellulose Nanofibers
[BMIM][Cl]	Butyl Methylimidazolium Chloride
CA	Carbon Aerogel
CNCs	Cellulose Nanocrystals
CNFs	Cellulose Nanofibers
Cp	Cyclopentadienyl
CMC	Carboxy Methyl Cellulose
CEC	Carboxy Ethyl Cellulose
DA	Diel-Alder
DMAc/LiCl	N, N-Dimethylacetamide Lithium Chloride
EDX	Energy Dispersive X-ray Analysis
FTIR	Fourier-Transform Infrared Spectroscopy
GLY	Glycerol
HPH	High Pressure Homogenization
HEC	Hydroxyethyl Cellulose
HECLLE	Hydroxyethyl Cellulose Lauryl Ether

HRP	Horseradish Peroxidase
HAD	Hetero Diel Alder
HPC	Hydroxy Propylmethyl Cellulose
HMW	High Molecular Weight
IL	Ionic Liquid
ILmCNFs	Ionic Liquid Modified Cellulose Nanofibers
ILCNFs	Ionic Liquid Cellulose Nanofibers
LCNFs	Lignocellulosic Nanofibers
LMW	Low Molecular Weight
MFC	Micro-fibrillated Cellulose
MW	Microwave
MC	Methyl Cellulose
mCNFs	Modified Cellulose Nanofibers
NFCs	Nanofibrillar Cellulose
NMR	Nuclear Magnetic Resonance
PABA	Para-Aminobenzoic Acid
PAM	Polyacrylamide
PCL	Polycaprolactone
PEEP	Poly Ethyl Ethylene Phosphate
PMMA	Polymer Methyl Methacrylate
PSD	Particle Size Diameter
PVA	Polyvinyl Alcohol Film
RAFT	Reversible Addition-Fragmentation Chain Transfer Polymerization
REO	Rosemary Essential Oil

SCB	Sugarcane Bagasse
SCS	Silyated Cellulose Sponges
SEM	Scanning Electron Microscope
SDS	Sodium Dodecyl-Sulfate
TBAB	Tetra Butylammonium Bromide
TEMPO	2,2,6,6-Tetramethylpiperidine-1-Oxyl
TEM	Transmission Electron Microscope
Tg	Glass Transition Temperature
TS	Tensile Strength
UV	Ultraviolet
WG	Wheat Gluten
WVP	Water Vapor Permeability
XRD	X-Ray Diffraction Analysis

Abstract

Cellulose, a ubiquitous and sustainable natural resource, exhibits significant promise as a substitute for synthetic and petroleum-based materials due to its abundant supply, biodegradability, and biocompatibility. Cellulose Nanofibers (CNFs), derived from sources such as sugarcane bagasse and *Eucalyptus* bark through mechano-chemical processes, offer impressive strength-to-weight ratios and eco-friendly attributes. This thesis aims to enhance CNFs' compatibility with the biopolymer, wheat gluten (WG), for the development of high-strength bioplastics. A microwave-assisted esterification process with para-amino benzoic acid (PABA) improved CNFs' dispersibility, solubility, surface properties, mechanical strength, and thermal stability. Evaluation through various tests, including Zeta-Analysis, FTIR, and UV-Visible spectroscopy, confirmed the success of CNFs production and modification.

The integration of CNFs and modified CNFs (mCNFs) as fillers into WG polymer films is poised to enhance mechanical properties, contributing to their structural integrity. Introduction of a thermally stable ionic liquid into CNF-infused WG films may further improve thermal stability. Characterization of the films encompassed solubility testing, FTIR analysis, and antimicrobial assays; revealing significant potential for sustainable biocomposite materials with versatile applications in industry.

CHAPTER 1

INTRODUCTION AND REVIEW OF LITERATURE

The most recent environmental issues have prompted a worldwide search for cleaner and more environmentally friendly materials. Researchers and scientists are motivated by the need to create environmentally friendly green materials using a variety of resources, such as non-petroleum-based chemicals, biodegradable cellulosic fibers from plants, and recyclable cellulose-based waste products [1]. Being the most abundant, cellulose is the most important biopolymer due to its vast applications. It is widely used due to its availability, sustainability, biological degradability, and biocompatibility. Cellulose is a polymer of glucose units joined together by beta, 1→4 glycosidic bonds, forming an unbranched polysaccharide molecule (Figure 1.1). It contains a unique hierarchy of structure: polysaccharide chains form cellulose nanofibers (CNFs), which range from 2-20 nm in diameter and a few micrometers in length; CNFs join together to form elementary fibrils, ~100 nm in diameter; elementary fibrils then form bundles with diameter in the order of 300 nm, called microfibrillated cellulose (MFC); and the cellulose microfibrils bundle up to make strands of cellulose fiber, ~100 μm diameter. The nanometer-sized fibrils are commonly known as whiskers, nanowhiskers, or nanofibers, while MFC is also called microfibrillated aggregates, and the cellulose fiber is also the commonly known plant fiber and dietary fiber [2, 3]. CNFs can be extracted from virtually any plant biomass; different resources have been used for CNF extraction such as cotton, wood fiber, prickly pear fruits, potato tubers, lemon, maize, soybean, wheat straw, soy hulls, hemp fiber, coconut husk fibers, pea hull fiber, mulberry, pineapple, banana peel, and sugar beet etc. [4]. With all of that, there are several options to get various CNFs, made even more numerous when we consider the range of raw materials that may be used to produce them, mostly wood but also other than plants; algae, bacteria, or tunicates [5]. Hardwood and softwood species make up the most researched category of plants. The hemicellulose and lignin content are a couple of the variances between these kinds of species. Mannose predominates in softwood while xylose is the most prevalent hemicellulose monomer in hardwood [6, 7].

The derivation of CNFs from renewable resources draws more attention towards material applications, because of their exceptional properties like strength-to-weight ratio and modulus of elasticity with large specific surface area, high aspect ratio, low coefficient of thermal

expansion, excessive environmental benefits, and more specifically low production costs [5]. Nanofibers have promising industrial applications in pharma, packaging and films, dietary food, the reinforcement in polymer matrices, specialty papers [6].

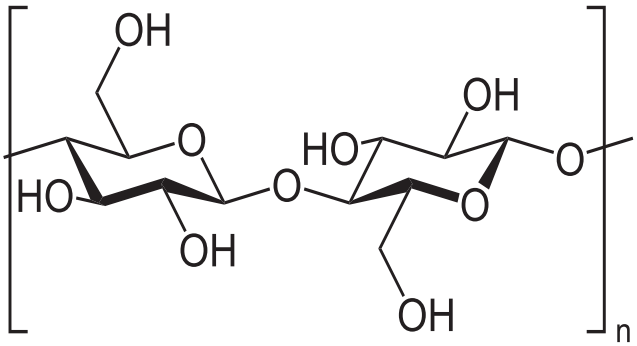

Figure 1.1 Cellulose, a linear polymer of β, D-glucose units linked by β, 1→4 glycosidic bonds [8]

Common mechanical treatments for the fibrillation of CNFs include cryocrushing, microfluidization, refining, grinding and high-pressure homogenization (HPH) [7]. All these techniques require a lot of energy to break the fibers' structure, and form poorly homogenized final product [9]. To tackle this problem, certain pretreatments are applied such as use of enzymes, chemicals or some chemo-mechanical ways [10]. In chemical treatment, 2,2,6,6-tetramethylpiperidine-1-oxyl (TEMPO) radical carboxylation of cellulose is carried out for their fibrillation (TEMPO-mediated), in the presence of NaBr catalyst and NaClO as an oxidant. It is an expensive approach to get high-quality, homogenized nanofibers [11, 12]. In chemo-mechanical pretreatment, dewaxing of cellulose is performed by Soxhlet Extraction by using ethanol/benzene mixture to break the hydrogen bonds and loosen the bonds between lignin, hemicellulose and cellulose [13]. In enzymatic treatment, the enzymes hydrolyze both crystalline and non-crystalline regions of cellulose, and give sharp and length-controlled nanofibers, for example, a mixture of endoglucanases and exoglucanases is used on *Eucalyptus* pulp [14].

After the fibrillation, the cellulose nanofibers are used for different applications, which depend on the method chosen for preparation. Different approaches provide different geometrical nanofibers of different diameters and lengths, and each has specific applications. CNFs are further modified to expand their range of applications. There are different methods to modify CNFs, i.e., chemical, physical, biological, electrochemical, and surface coating modifications.

Among all these modifications, chemical modification is the most employed. Cellulose is difficult to dissolve in common solvents; its rich hydroxyl groups make it hydrophilic in nature, which constrains its applications [15, 16]. Among the chemical modifications, oxidation, esterification, etherification, and graft copolymerization are most common.

Cellulose derivatives such carboxymethyl cellulose (CMC), methylcellulose (MC), and cellulose acetate are implemented in many fields and applications, such as in pharma and food industry. Modification of polysaccharide hydroxyl groups with hydrophobic groups effectively breaks the hydrogen bonds network and increases cellulose solubility in organic solvents. These modifications also impact its thermoplastic properties [17, 18].

In **oxidation technique** of cellulose modification, electrocatalytic oxidation approach was used by which cellulose was converted into gluconate by using pretreated conc. HNO_3 carbon aerogel (CA) in an alkaline medium, on which gold (Au) nanoparticles were supported as anode. Results showed high gluconate yield of 67.8% and total yield of salts can be obtained up to 88.9% after 18 hours of hydrolysis. It was a key success to convert cellulose into gluconate by using electrolytic oxidation in alkaline medium [19]. In **etherification**, a secondary reaction was performed on pre-treated hydroxyethyl cellulose (HEC). HEC and 1-bromododecane (1-BD) reacted in the presence of tetramethylene oxide and water as solvent, to produce hydroxyethyl cellulose lauryl ether (HECLLE), while tetrabutylammonium bromide (TBAB) was used as phase transfer agent [20]. Eco-friendly **graft polymerization** to modify cellulosic material was performed by combining enzymatic catalysis and reversible addition-fragmentation chain transfer polymerization (RAFT). By using RAFT and horseradish peroxidase (HRP), polyacrylamide (PAM) was polymerized on filter paper surface with promising results [20]. Another eco-friendly and solvent free method to graft the CNFs by using **Ultraviolet (UV) rays**. UV rays generated radicals on CNFs surface and provided the sites for polymer grafting, methyl methacrylate (PMMA) was readily grafted on the surface of CNFs without causing harm to original crystalline structure of cellulose. These grafted CNFs showed unique structure in water, improved re-dispersibility and hydrophobicity in organic solvents [21].

Esterification processes, in which an acylating agent combines with cellulose nanofiber hydroxyl groups, is a method frequently used to make the surface of cellulose more hydrophobic. It is possible to esterify cellulose nanofibers using homogeneous or heterogeneous methods [22]. In homogeneous method esterified cellulose fibers are solubilized in the surrounding solvent and easy to derivatize due to complete diffusion of its branches in

the medium [23]. In heterogenous method the medium is nonsolvent for both native as well as for cellulose and the original morphology of CNFs are preserved [24]. Cellulose microfibrils obtained from wheat straw fibers were subjected to esterification by propionylation by varying the time, temperature, and concentration conditions. These fibrils were then homogenized to get surface modified CNFs. Effects were investigated by using Fourier-transform infrared spectroscopy (FTIR), energy-dispersive x-ray spectroscopy (EDX), scanning electron microscopy (SEM), transmission electron microscopy (TEM), X-ray diffraction (XRD), elemental analysis, and static and dynamic incidence angle measurements. FTIR confirmed the propionylation [25]. **Carboxymethylation** of bacterial cellulose nanocrystal (BCNCs) and bacterial cellulose nanofibers (BCNFs) to improve its solubility in polar media also shown promising results [22, 26].

Protein-based materials have been investigated as viable packaging materials due to their effective barrier qualities against (dry) oxygen and aroma chemicals [27]. From a materials science lens, proteins are thermoplastic heteropolymers containing both non-polar and polar amino acids that can form a great number of intermolecular connections and undergo a wide variety of interactions, providing a large range of potential functional capabilities [28]. Wheat gluten (WG) is considered as one of the many protein sources that have been suggested for the creation of biodegradable films due to its intriguing viscoelastic and film-forming properties; capacity to make cross-linkages when provided with heat, low water solubility, cost effectiveness, and accessibility as an industrial byproduct of the wheat flour [29, 30].

To create novel materials with minimal environmental impact, a lot of research has been done. Particularly, biopolymer composites and nanocomposites with natural fillers appear to be promising as green structural materials [31]. Owing to the exceptional qualities of cellulose for application in composites, renewability and biodegradable nature, cellulose nanofibers have been used to strengthen biopolymer films. In recent research, there has been a focus on creating biopolymeric composites with enhanced characteristics reinforced with natural nano-based filler materials [32]. Wheat gluten has comparatively low cost, large abundance, quick biodegradability, and favorable film-forming qualities, and is one of the most promising renewable materials for the manufacturing of bioplastics. Furthermore, it is available as an industrial byproduct. When dried, wheat gluten films display strong barrier qualities against gases (including oxygen, carbon dioxide, and fragrance chemicals). Because the wheat gluten film is fragile, many techniques have been employed to change it, such as adding plasticizers and cross-linking agents. Due to its advantageous characteristics, such as biodegradability,

being a natural, plentiful supply with a low cost, low density, and high mechanical strength, cellulose nanomaterials can be employed as a high-performance fillers for bioplastics [33]. The aim of our study was to add modified CNFs in wheat gluten to make gluten composites with enhanced properties.

1.1 Nanocellulose

The most prevalent biopolymer on earth, cellulose has a high molecular weight and a hierarchical structure. Its annual production can reach up to 10^{11}-10^{12} tons. This homo-polysaccharide, semi-crystalline, linear structure is created by repeatedly attaching β-D-glucopyranose monomers with β-1,4-glycosidic linkages at 10,000–15,000 degrees of polymerization [34]. It is possible to shrink it to nano-scaled fibers (where at least one dimension is < 100 nm). Similar to other nanomaterials, nanocellulose exhibits completely unique features relative to its bulk size, including chemical, physical, and biological ones [35]. The formation of nanoscale structures in cellulose occurs spontaneously during its manufacture, when glucan chains (up to 100) combine to form primary fibrils or nanosized cellulose fibrils. Higher surface area, tensile strength, modulus, stiffness, piezoelectricity, surface reactivity, heat resistance, aspect ratio, and light transparency are only a few of the distinctive qualities that nanocellulose has over cellulose [36].

1.2 Cellulose Nanofibers (CNFs)

The term "Cellulose Nanofibers" refers to cellulose fibers that are long (up to several micrometers) with 10-100 nm in diameter, flexible, and interlaced in a web-like pattern. which are made up of two portions: crystalline and amorphous [37]. First name of CNFs was nanofibrillated cellulose (NFC) used by Turbak, Snyder and Sandberg in 1970s. Other names of CNFs in the literature are microfibrillated cellulose (MFC) and cellulose nanofibers (CNFs). The primary variables that have a significant impact on the diameter, length, and yield of CNFs are their sources and techniques of production, which lead to a wide variability in the fundamental CNF characteristics [38].

There was little interest in the commercial manufacture of CNFs since the first conception of the idea, because it required significant energy input (between 12000 and 65000 kWh/ton). However, in recent past, following the introduction of various chemicals for example, TEMPO, carboxymethylation, periodate, alkalis and acids (HNO_3, H_2SO_4, HCl), and enzymatic (endoglucanase) pretreatments, the interest for commercial production of CNF has returned because of the notable decrease in energy consumption (500-1500 kWh/ton) after pretreatments [14].

1.3 Manufacturing of CNFs

CNFs are mostly produced through chemo-mechanical method in which chemical processes are followed by some mechanical approach for the fibrillation of cellulose (Figure 1.2**)**. **Milling** is the starting step, in which the biomass source is crushed to fine form by using ball mill or a grinder, followed by washing. Milling is used to reduce fiber size, improve contact surface, swelling property and uniformity, and washing is used to get rid of contaminants. Sometimes **dewaxing** of the sample is also employed before washing, by using benzene: ethanol and toulene: ethanol solutions. Dewaxing eases the removal of lignin and hemicellulose from the sample by weakening their bonds. The terms "**purification step**" often apply to the traditional pulping and bleaching processes. The primary goal of purification is to eliminate as much hemicellulose and lignin as possible, from cellulosic material since they both serve as protective coverings for cellulosic fibrils and provide barriers to their separation. Kraft and sulfite are two famous approaches in purification/ pulping. In Kraft pulping, NaOH and Na_2S are used to remove lignin and hemicellulose. In sulfite pulping, sulfurous acid (H_2SO_3) is used. Apart from these, many researchers have used other methods; the use of NaOH or KOH at high dose to remove any fat, pectin, lignin, and hemicellulose from softwood as well as hardwood. **Alkaline treatment** is often intended to aid in cellulosic fiber/ cell wall swelling, to improve the softness and surface area at low dosages. The remaining lignin is eliminated using various bleaching agents, such as $NaClO_2$, NaClO, and ozone (O_3) in an acidic environment; and hydrogen peroxide (H_2O_2) and glycolic acid ($C_2H_4O_3$) in an alkaline environment [39]. The same procedure is repeated to eliminate most of the lignin.

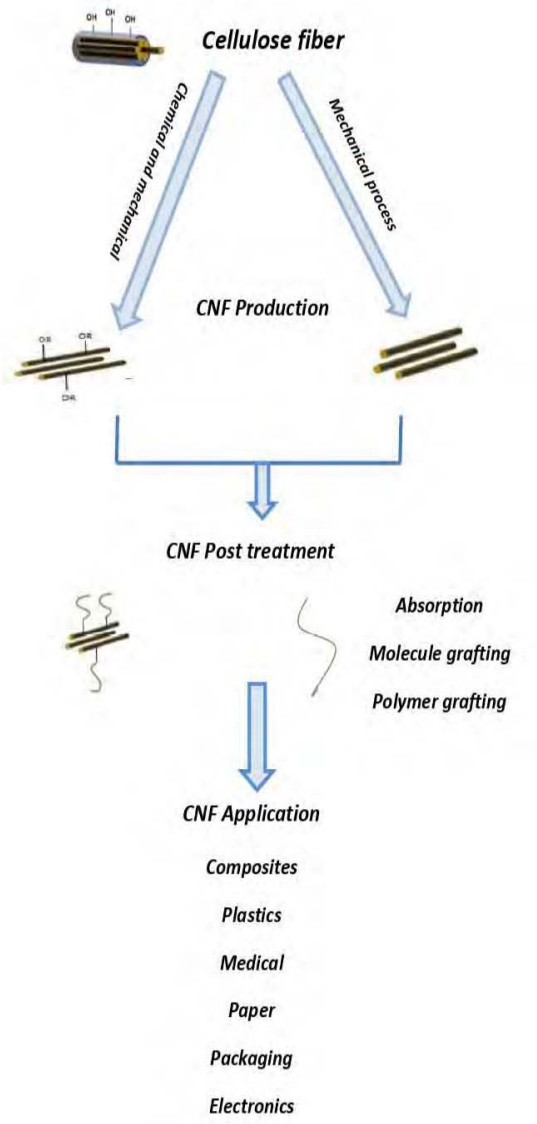

Figure 1.2 Short summary of cellulose production, modification and uses.

1.4 Pretreatments

Pretreatment of pure cellulosic feedstock is an important step of the procedure, to decrease the vitality demand during mechanical dissolution of cellulose nanofibers. According to some researchers, directly using mechanical action for nanofiber segregation, without any pretreatment, is an energy-concentrated approach. Table 1.1 outlines the pretreatments used the production of cellulose nanofibers.

Table 1.1 Summary of different pretreatments found in literature [39].

Pretreatments	Chemical/Enzyme	Effect	Reference
TEMPO- mediated oxidation (carboxylation)	2,2,6,6-tetramethylpiperidine-N-oxyl/ NaBr/ NaClO	Induces negative charges, causing repulsion between fibers	[40]
Carboxymethylation	Isopropanol and ethanol mixture. Aqueous NaOH solution and Chloroacetic acid		[41]
Sulfonation	Sodium periodate ($NaIO_4$) and sodium bisulfate ($NaHSO_4$)	Induces negative sulfate groups that cause repulsion between fibers	[42]
Quaternization	EPTAC (2-3-epoxypropyl trimethylammonium chloride), Glycidyl trimethylammonium chloride (GTMAC), Isopropanol (C_3H_8O), Sodium hydroxide (NaOH)	Induces positive charged ammonium groups, causing repulsion between fibers	[43]
Deep Eutectic Solvent (DES)	Choline chloride and Urea	Causes fiber separation	[44]
Organic acids	Maleic acid, sulfonic acid, p-toluene, and oxalic acid	Induces fiber separation	[45]

Base + Acids	NaOH followed by HCl	Exploration and separation of cellulose nanofibers	[46]
Enzymes	Exoglucanases and glucosidases	Hydrolysis of cellulose causes separation and delamination of cell walls	[47]
Solvo-thermal	Peroxide, ethanol, sulfuric acid	Disintegrates lignin and hemicellulose	[45]

1.5 Mechanical Treatments

Cellulosic biomass that has already undergone purification and pretreatment is subjected to intense mechanical or physical processing, to further shrink it down to nanoscale fibers (Figure 1.2). Without the use of mechanical force, it is impossible to separate the nanofibers present in cellulose, because they are so thoroughly whole, entangled, and bound by hydrogen bonding and Van der Waals connections [48]. Mechanical pressures result in the delamination and fibrillation of the fibers, separating the nanofibers. Pretreatment confers on cellulose fibers a variety of distinctive properties, including increased surface area, hydroxyl groups exposure, altered crystallinity, altered surface area chemistry, and decreased hydrogen bonding [49].

Table 1.2 Different mechanical treatments for cellulose disintegration.

Mechanical Treatment	Description	References
Homogenization	High pressure homogenizer (HPH): It provides constant volume, pressure change, high shear force, random flow, and collision between particles, which convert cellulose fibers into NFs. Microfluidizer: Works at constant shear rate, provides high pressure and velocity. Produced shear and impact forces cause the disintegration of cellulosic fibers.	[50-52]
Grinding	Super mass collider-grinder Gap between the discs is adjustable, and shearing forces produced between the discs cause cellulosic fibers to transform into nanofibers. It is possible to process high consistency fiber suspension (2-5% w/v). To encourage the fibrillation and individualization, corrosive fillers may also be utilized. No clogging problem.	[53, 54]
Refining	Valley beaters, PFI mills, and disc refiners	[51]

	Shearing and cutting actions result in the conversion of cellulosic fibers into nanofibers, repetitive loading of bars peels away cell wall layers, and a rise in fines. Used often for mechanical pretreatment.	
Extrusion	By peeling off cellulosic fibers using co-rotating screws that are intermeshed and framed in a barrel, cellulosic fibers are transformed into nanofibers. Nanofibers (powder form), capable of operating at high fiber consistency (25–40% w/v) It is conceivable for in-situ fibrillation to occur whilst composite creation. Low manufacturing costs because of speed and effectiveness High uniformity of fibers, prolonged friction, elevated temperatures, and kneading and breaking activities throughout the process might cause irreversible clusters of nanofibers), deterioration, and other problems.	[55, 56]
Blending	Modified domestic mixer-grinder. Fiber alteration occurs because of cutting and shearing processes (simplified at the micro to nano level). Lessen fiber damage, although ineffective (only a small amount of undamaged fibers is left). Homogeneous suspension of micro/nanofibers.	[57]
Ultrasonication	Cellulose fibers are transformed into nanofibers by the hydrodynamic shear stresses of ultrasonic oscillation. Ultrasonic energy was used to create loud cavitation and implosive implosion (hot spots) through tiny gas. Delamination of the fiber walls occurs when the hydrogen-bond connection between the cellulose fibrils and nanofibers is destroyed.	[45]

Cryocrushing	Water-swollen cellulose fibers that have been frozen in liquid nitrogen and then mechanically crushed (either with a mortar and pestle or a grinder) Due to resistance and pressure from crystals of ice in the form of nanofibers, fines, and fragments, cell wall fragments that are hidden or covered up are now revealed. Mostly employed for producing nanofibers from agricultural waste and crops	[58]
Ball milling	A hollow cylinder is filled with different-sized balls (made of metal, ceramic, or zirconia). By means of cyclic deformation brought on by friction and the grinding action of high-energy collisions among the progressing balls, cellulose fibers are transformed into nanoscale fibers. It is feasible to process fibers with a high consistency (50%) Decrystallization may result from uncontrolled milling.	[59]
Aqueous counter collision	When cellulose fibers in a water-based mixture are fed via two nozzles at high pressure (50–270 MPa), they impact at an angle of 170° to get pulverized into nanoscale filaments. The yield of nanoscale fibers can be almost 100%. Usually, cellulose nanofibers with a larger surface area and a smaller aspect ratio and length are produced. If the fiber size of the suspension is larger than micro scale, clogging may occur.	[59]

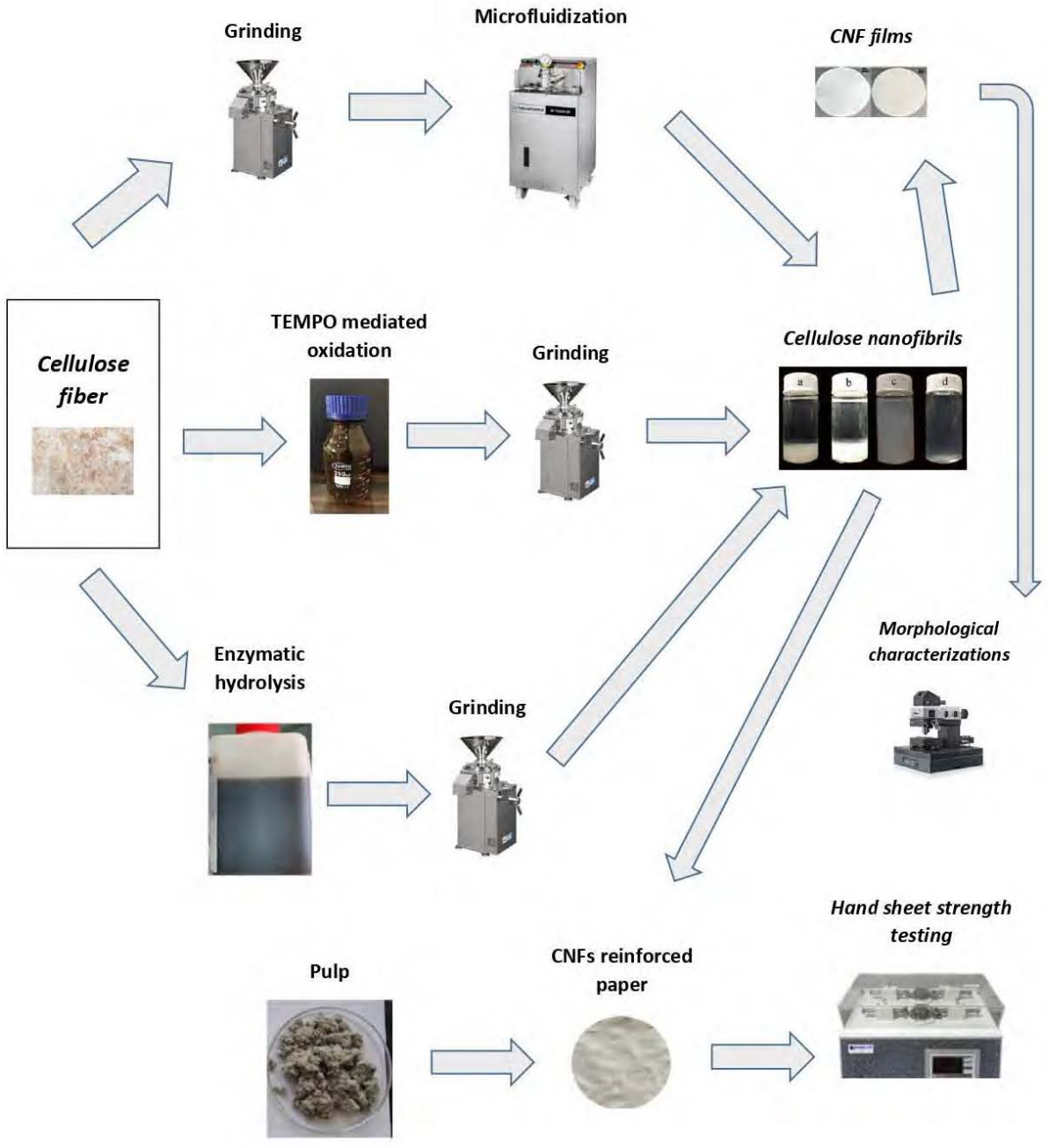

Figure 1.3 Cellulose nanofibrillation by using different mechanical approaches.

1.6 Modification of Cellulose Nanofibers

The building blocks of cellulose are recurring anhydrous glucose units (AGU), which are bonded together covalently by recurring cellulose OH group units found in acetal functions. It is simple to alter the primary surface OH groups along molecule chains by interacting with them. An extensive spectrum of cellulose derivatives is produced [60]. The steric effect of chemicals and supramolecular structure both affect the wide spectrum of reactivity of AGU [61]. Solvent systems have been utilized to produce cellulose derivatives through the processes of esterification, acylation, grafting, and etherification [62, 63]. Due to its high availability, renewability, and biodegradability, cellulose becomes an attractive contender to produce sustainable products [64].

In their natural condition, cellulose-based bioproducts have difficulty displacing synthetic polymers. These difficulties include problems with scalability, high manufacturing costs and the limited utilization of cellulose-based materials. Cellulosic materials must have qualities that are suitable for the end user and perform to expectations to compete with synthetic polymers. In this way, surface modification of pre-made cellulosic materials maintain the chemical composition, mechanical characteristics, and biodegradability of cellulose while broadening the range of potential uses. A variety of chemical alterations have been made to cellulose to increase its utility in several different industries [39]. These alterations, which ranged from simple molecules to polymers, either altered the chemistry or added specific functional groups to CNFs surface. Among many other chemicals, aromatic and aliphatic mono and di-isocyanates are a class of compounds that have been applied to cellulose modification for a century.

1.6.1 Surface Modification of Cellulose

Due to its OH groups, surface modification of cellulose considerably boosted its potential; nonetheless, it is challenging to manage the interaction between cellulose and the di-isocyanate [65]. There are following modifications quoted in literature.

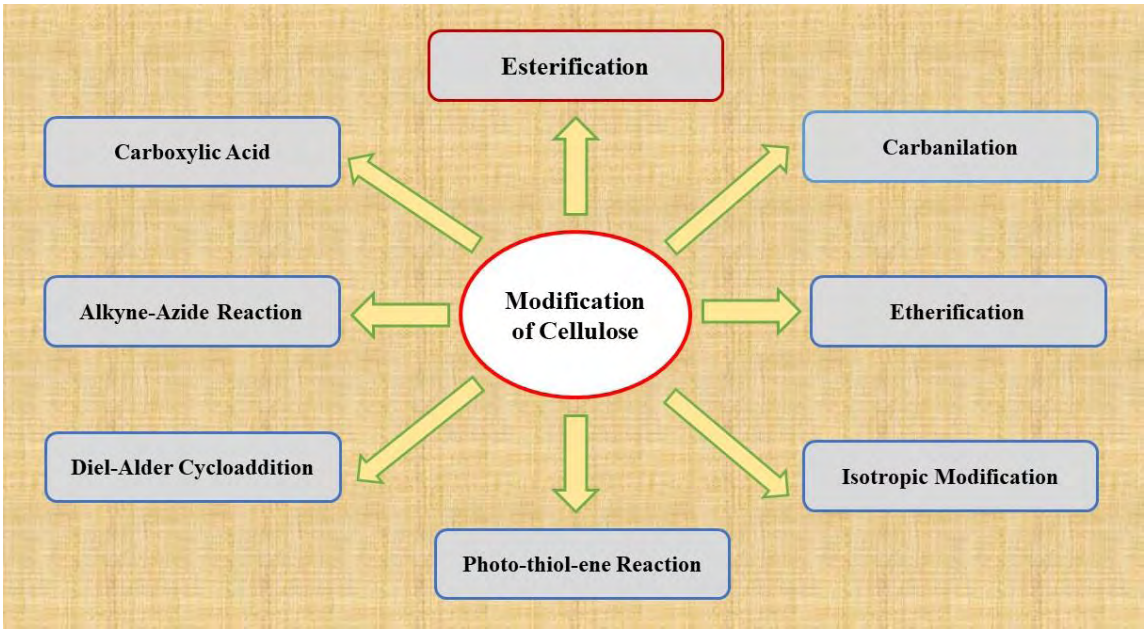

Figure 1.4 Possible modifications of Cellulose found in the literature.

1.6.2 Modifications by using Carboxylic Acids Groups

CNFs which are **TEMPO** oxidized contain a rich amount of carboxylic active groups on its surface and make it ideal for functional modifications. Fluorophores are routinely attached to TEMPO-oxidized cellulose via the reaction with Lissamine Rhodamine B Ethylenediamine. The production of N-hydroxysuccinimide, an activated ester, as an intermediate is crucial. The TEMPO-oxidized cellulose may be immediately functionalized using the nitrile imine carboxylic acid (tetrazole-based) ligation technique [47, 66]. By using an azetidinium salt and H_2SO_4, cellulose is isolated. Indirect surface modification necessitates pre-modification. The added functionality is frequently the result of the functional group's increased activity. Either one step or two steps might be included. Multiple functional groups, including different dyes, can be introduced using two-step processes. Depending on how the cellulose is isolated, carboxylate functionalities may not be present. Then, amine groups can be introduced to a pairing process between the activated esters of the amines. The technique has been used multiple times in order to glue fluorescent dyes on cellulose [67].

1.6.3 Modification by Alkyne-Azide Reaction

The addition of an alkyne functionality causes cellulose surface to respond. The OH groups of cellulose react with 1-azido-2,3-epoxypropane at room temperature. The propargylic groups, such as propargyl-modified 4,6-dichloro-1,3,5-triazine and propargylamine, can also be produced to do this. Investigated was the common interaction of cellulose with poly (ethyl

ethylene phosphate) PEEP and poly(e-caprolactone) PCL by using active catalyst e.g., copper [68, 69].

1.6.4 Modification by Diel-Alder Cycloaddition

The effectiveness of Diels-Alder (DA) reactions in the presence of additional functional groups makes them desirable. Modifying maleimide-modified cellulose with useful compounds is simple. Different colors are used to tag cellulose for its biological monitoring. Under moderate, rapid, and modular circumstances, hetero Diels-Alder (HDA) cycloaddition was combined with RAFT polymerization. A solid cellulose substrate was grafted using poly (isobornyl acrylate) [70]. The active -OH linkages on the cellulose fibers were changed into tosylate leaving groups, and then a highly reactive Cp (cyclopentadienyl functionality) was added to replace it. By exploiting the reactive Cp-functionality as a diene, an HDA cycloaddition was used to link the surface of the isobornyl acrylate generated by RAFT polymerization (started by benzyl pyridine-2-yldithioformiate, or BPDF) to the thiocarbonyl thio-capped poly (isobornyl acrylate). The analytical outcomes offer convincing proof that, under moderate reaction circumstances, an effective reaction between appropriate dienophiles and Cp-functional cellulose occurs. A homogenous dispersion of the polymer coating is visible on the cellulose fibers when individual modified cellulose fibers are seen [71].

1.6.5 Modification by Photo-thiol-ene Reaction

Surface-modified cellulose has predominantly been produced by these radical-containing processes. Recently, they have been investigated to create drug carriers made of water-cellulose. A nitrile imine that is light-driven, mediates the cycloaddition of tetrazole-ene. A promising light-induced ligation is one like this. It serves as a companion for non-activated alkenes. Depending on the structure, fluorescence of the resulting pyrazoline cycloadduct alkenes revealed different emissions, such as 487-538 nm. It is among the most alluring features of this kind of response. This makes it possible to produce cellulose with integrated fluorescence [16], enabling direct material monitoring in a biological environment [72].

1.6.6 Isotropically Modified Cellulose

Amines can react with grafting on terminal groups that change the final functioning in a ring-opening process [73]. Just like cellulose, the terminal group of carboxylic acid and polysaccharides can be impacted selectively. The functional end of cellulose may be attached to a variety of scaffolds; this approach allows the cylinder-shaped cellulose to be bonded to a

surface merely by the base. This made several unusual structures possible. Following the oxidation of reducing end functionality, biotin was attached by amidation to create cellulose with four arms by binding to its binding sites [74]. These modifications are extremely promising for the very effective heat dissipation of a variety of electronic devices because they have great mechanical strength, super flexibility, superb transparency, and outstanding electric insulation.

1.6.7 Modification by Etherification

Due to their initial basicity, alkaline aqueous solutions are perfect for the generation of cellulose ethers since they may serve as homogeneous reaction medium [75]. Cellulose ethers have so far been synthesized in alkali aqueous systems, including hydroxyethyl cellulose (HEC), methyl cellulose (MC), carboxymethyl cellulose (CMC), carboxyethyl cellulose (CEC), and hydroxy propyl methyl cellulose (HPC). Basically, etherifying agents like epoxides and alkyl halides are used to react to create these derivatives [76]. Through temperature-induced thiolene, silylated cellulose sponge (SCS) can subsequently be functionalized with different thiol-containing substances like 3-mercaptopropionic acid. At 80% compression strain, the hydrophilic cellulose sponge demonstrated good mechanical strength of 70 KPa. The produced sponge was employed in gravity-driven removals of oil-in-water emulsions with a good separation efficiency because it had underwater oleophobic and hydrophilic qualities [55]. Alkali cellulose also offers a perfect setting to produce cellulose-based hydrogels because of its high-water content and strong dissolving properties [77]. These hydrogels are created by chemically cross-linking cellulose derivatives. Cellulose hydrogels were produced using 1,4-butanediol diglycidyl ether (BDE) in a solution of 6 weight percent NaOH and 4 weight percent urea [78]. With the help of allyl glycidyl ether (AGE), cellulose is etherified to create double bonds by chemical cross-linking, resulting in the creation of cellulose ionic hydrogels with great elongation [79].

1.6.8 Carbanilation

Isocyanate can be used as a reagent to achieve the carbanilation of cellulose. *Heinze et al.* showed three distinct degrees of carbanilation polymerization with cellulose in 1-butyl-3-methyl-imidazolium chloride [BMIM][Cl]. Phenyl isocyanate was used to carry out the reaction in the absence of catalysts. Using 10 anhydrous glucose units, fully substituted cellulose carbanilates were produced at 80 °C for 4 hours. Bacterial cellulose, which differs greatly from plant cellulose, received the carbanilation [80].

1.6.9 Modification of Cellulose by Esterification

The multiple hydroxyl groups that CNFs have on their surface contribute to a complicated network that is sustained by many hydrogen bonds [62]. Due to the crystalline structure caused by these interactions, CNFs are insoluble in organic solvents and water at room temperature [81]. To address the rising demand for environment friendly goods, the surface with hydroxyl groups enriched represents a fertile ground for the development of functional materials. The most renowned chemical modification processes that has been used extensively to change the structure of cellulose, is esterification [82]. The hydroxyl groups on CNFs are reacted with by an acylating chemical to form ester groups in this process. To get the appropriate characteristics for the application, the surface of CNF was esterified using acid anhydrides [81], acyl chlorides [83], or carboxylic acid [22]. According to *Sehaqui et al.,* a wide range of carboxyl-functionalized CNFs with improved thermal stability were produced by esterifying wheat fibers by using different cyclic anhydrides (maleic, phthalic, and succinic) [84]. *Chhajed et al.* discovered super hydrophobic cellulose nanofibers with high porosity, made from stearic acid chloride, to be extremely selective as a superabsorbent for organic pollutants and oils, in the case of the esterification utilizing acyl chlorides reagents [83]. Research on the surface modification of CNFs using valeric or hexanoic acid was just completed by Her et al. [85]. These esterified CNFs exhibit greater hydrophobicity, allowing for their dispersion in nonpolar organic environments, as a result of the recently grafted alkyl side chains [86].

Recently, it has been claimed that a CNFs esterification process run on microwave (MW) energy can be both economically and environmentally sustainable. The polar nature of molecules and their capacity to absorb and convert microwave radiation into heat constitute the basis of the MW heating theory. The MW heating method proven to be effective, uncomplicated, solvent-free, and clean. *Joly et al*., for instance, reported that MW irradiation was used to esterify cellulose using acyl chloride derivatives, which resulted in a reaction time reduction from several hours to only 30 minutes [87]. *Semsarilar et al.* explored how MW irradiation helped dissolve and functionalize cellulose in the N,N-dimethylacetamide lithium chloride (DMAc/LiCl) system [88]. Similar work was also done by *Farida Bakara et al.,* in which they used MW assisted technique to esterify the CNFs surface by using bleached and unbleached fibers. They used sulfuric acid assisted para-amino-benzoic acid to esterify aliphatic hydroxyl groups of CNFs. Nuclear magnetic resonance (NMR) and FTIR showed positive results. By integrating ester and aromatic amine functionalities, this environmentally

friendly chemical approach may improve the utility of CNFs, creating LCNF-E and CNF-E sustainable platforms for more intelligent applications [86].

1.7 Wheat Proteins

There is 8-10% protein content in the wheat grains. Among these proteins, Albumin and Globulins constitute around 15-20% and the remaining 80-85% consist of Gluten.

1.7.1 Gluten

The stretchy mass produced when starch is removed from flour with a water stream is known as wheat gluten (WG). The majority of WG is made up of storage proteins, made up of around 100 different proteins which are either polymeric or monomeric [89]. Gluten proteins are unique proteins due to their composition, being rich with proline and glutamine with low amount of charged amino acids. Unique structural and functional properties come from high amount of cysteine residue which helps in the formation of both inter- and intra-molecular disulfide crosslinks. The gluten proteins have distinguished properties over the proteins of other cereals like its elasticity, viscosity, and strength. Viscoelasticity is responsible for films formation ability, which is why they have been exploited in packaging films [89].

1.7.2 Composition of Gluten

Gliadin and glutenin are two major subgroups of gluten proteins. Monomeric gliadin is further sub-classified into three protein types and polymeric glutenin into two protein types as shown in Figure 1.5.

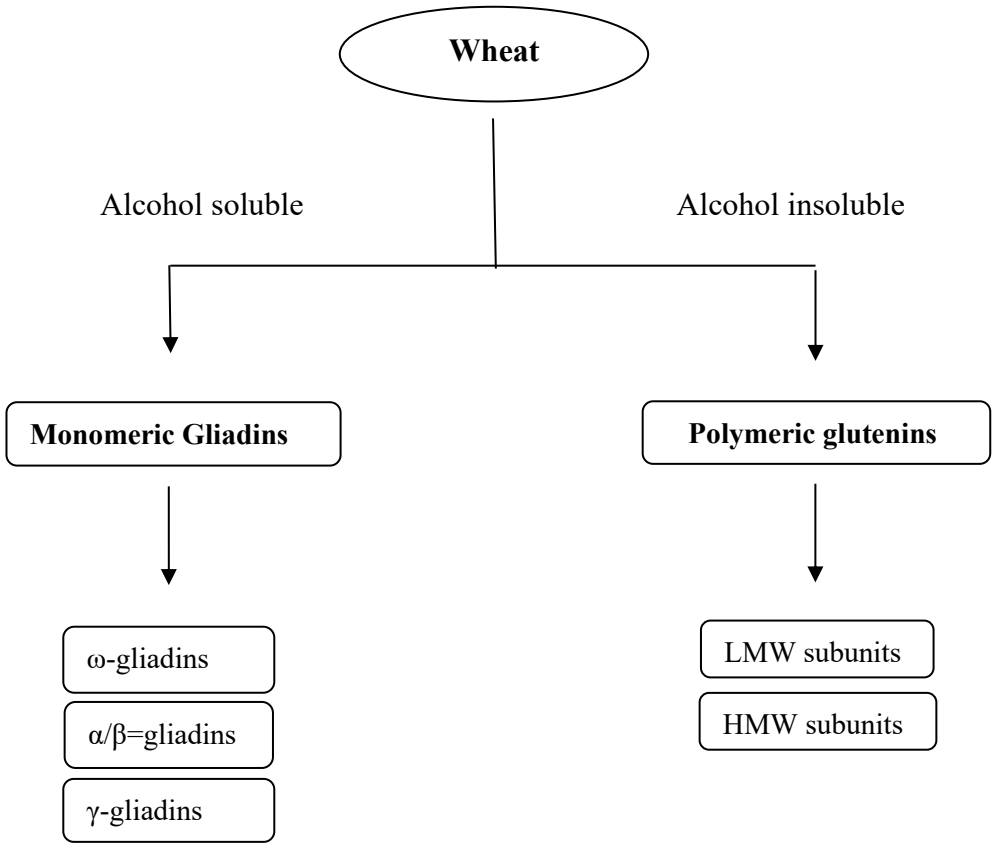

Figure 1.5 Basic composition of wheat gluten [89].

Alternatives to conventional plastics based on petroleum, that are created from naturally found polymers may be sustainable. Therefore, in past few years, research focus has shifted to creating edible and/or biodegradable packaging manufactured by using natural polymers, frequently from byproducts of agriculture or fisheries. The physical characteristics of the resultant films might vary greatly depending on the kind of polymer used, and such polymers may be based on lipids, proteins, or polysaccharides. Protein-based materials have been investigated as viable packaging materials due to their excellent barrier characteristics against oxygen (dry environments) and fragrance chemicals [33]. A lot of research has recently been put into creating novel materials with minimal environmental effects. Particularly promising as green building materials, are the composites and nanocomposites made of biopolymers and natural fillers [31, 90]. Despite their high economic potential, starch-based composites have

some flaws in their thermal, mechanical, and barrier characteristics [91]. Recent years have seen increasing potential for the scaled-up manufacturing of biodegradable materials (relying upon natural renewable resources), because of rising fossil energy costs and environmental considerations. Materials made from cheap and readily available proteins like wheat gluten have been successfully manufactured. These substances do not dissolve in water [92], are totally biodegradable and have high mechanical characteristics [93]. Commercial WG has undergone processing to create a variety of bio-based products, including films, adhesives, and foams [89]. The WG-based materials have proven to offer functionally appealing characteristics, such as oxygen barricade for films and flame retardant and drip-resistant capabilities for foams. When made into biobased films, the mechanical and barrier characteristics of the gluten proteins have been discovered to be influenced by their structure. The performance of bio-based films in terms of mechanical and oxygen barrier qualities has been reported to be enhanced by hierarchical structure arrangement of gluten into hexagonal and tetragonal assemblies [89].

1.7.3 Addition of Plasticizer

Amorphous gluten-based polymers may be created utilizing typical thermoplastic manufacturing techniques like extrusion or thermomolding [94, 95]. Polar but small molecules like water, glycerol ($C_3H_8O_3$), sorbitol ($C_6H_{14}0_6$), or fatty acids are used to plasticize materials [94, 96]. It improves the material's processability and lessens the brittleness of the finished product. WG degrades at a lower temperature than synthetic polymers, hence its processing at temperatures above 150 °C is avoided [97, 98]. Plasticizers enable processing at lower temperatures, hence reducing the energy input, by lowering the gluten glass transition temperature (*Tg*), 187 °C (for dry gluten) to around 124-145°C, along with the viscosity in the rubbery condition. The final material qualities are also impacted by the plasticizer. The stiffness and elasticity modulus of the material drop as the plasticizer concentration rises, whereas the elongation at break rises [99, 100]. Thus, the ideal plasticizer concentration strikes a balance between the demands of the manufacturing process and the required stiffness of the material [101].

1.7.4 Biocomposites

The basic benefits of employing plant fiber rather than synthetic fiber to strengthen biomaterials are forming a completely "green" material that may be described as 100% renewable [102]. A biocomposite is a substance composed of two or more separate constituent

materials, at least one of which is derived naturally, that are combined to make a substance that is more effective than the sum of its parts [103]. Interesting functional characteristics, such as viscoelasticity and water resistance, are displayed by materials derived from gluten. Materials made of gluten can have their mechanical characteristics changed according on the production parameters, such as temperature [97, 104] or mechanical energy input [105], or the composition of blend, such as by changing the plasticizer [76] concentration or by adding natural fibers [101, 102]. Fiber-integrated composites expand the range of applications for these materials, including the automotive and packaging industries. Natural fibers are eco-friendly, sustainable, affordable, have low density, with appreciable mechanical properties, separation simplicity, carbon dioxide sequestration, and biological degradation. That is why natural fiber-reinforced composites, such as those made of kenaf, jute, flax, sisal, hemp, and henequen fiber, are interesting research topics [106, 107].

1.7.5 Temperature

A study assessed how thermo-molded biodegradable WG polymers that have been plasticized with glycerol, are affected by the molding temperature. In relation to the molding temperatures, moisture absorption characteristics (tensile strength and elongation at break), crosslinking density, and stress relaxation were assessed. For elucidating the impact of molding temperature on the protein network structure further, dynamic mechanical analysis was carried out. The crosslinking density of the three-dimensional protein network, is greatly improved by molding at temperatures between 25 °C and 125 °C, thanks to the disulfide bonding of cysteine residues, which also boosts tensile strength, Young's modulus, and relaxation time [104].

1.7.6 Mechanical Energy Input

Using size exclusion high-performance liquid chromatography (SE-HPLC), blends of wheat gluten and glycerol that had undergone various thermal treatments were analyzed. To track the solubility loss of protein fractions with certain molecular sizes, the elution profiles were examined. Protein denaturation was split into two different reaction stages using a mechanistic mathematical model: (**a**) reversible change in protein structure, and (**b**) protein precipitation by disulfide bonding between originally SDS-soluble and SDS-insoluble fractions. This was done in response to the known biochemical changes involved during the heat denaturation of gluten. Using the Arrhenius law, the activation energies for the unfolding, refolding, and precipitation of gluten were determined to be 53.9 kJ/mol, 29.5 kJ/mol, and 172 kJ/mol, respectively. The development of a three-dimensional network that gradually hampered the cross-linking

process, might be the reason why the protein solubility rate loss decreased as the reaction progressed. Due to the larger proportion of cysteine residues in WG, and higher percentage of unfolded and subsequently activated proteins—complete protein refolding appearing to be an uncooperative process—large molecules were shown to be more susceptible to aggregation [105].

1.7.7 Addition of Natural Fibers

To create biocomposite, natural fibers—that are mostly made of cellulose, lignin, and hemicellulose—are frequently employed as integration. The plant from which the fiber is collected, as well as the agricultural practices, determine the fiber's composition. It is mostly made up of three substances: cellulose, lignin, and hemicellulose. Polysaccharides include cellulose and hemicellulose. While lignin is a three-dimensional, amorphous, polyphenolic macromolecule that is complicated, heavily branched, and comprised of three different kinds of phenylpropane units [108]. Due to its ability to form films, WG is an intriguing plant ingredient to be utilized in the creation of plastic-like polymers. Composite materials with enhanced mechanical qualities are required to be used as plastics in a wider range of applications. Plant fibers are mostly used in soy-based bioplastics and are currently very infrequently used as reinforcement for bioplastics [109].

1.7.8 Gluten mixed with Cellulose Fibers

The production of bio-based polymeric materials has attracted a lot of interest, and cellulose is the best prospective feedstock for this. During the last 10 years, significant progress has been achieved in the production of biopolymers based on diverse cellulose types. The use of cellulose fibers, nanocellulose, and cellulose derivatives as fillers or matrices in biocomposite materials is a cost-effective and environment friendly way. In addition to providing practical substitutes for many petroleum-based polymers, the use of cellulose-derived monomers (glucose and other platform chemicals) to synthesize sustainable biopolymers and functional polymeric materials enables the development of novel polymers and functional polymeric materials. In addition to replacing current petroleum-based polymers, sustainable cellulosic biopolymers may also be used to create cellulose functional polymeric materials for a variety of applications, including electrochemical and energy-storage devices as well as biomedical ones [18]. In some recent studies the CNFs and CNCs from different plant sources were used with gluten plastics, to make them completely natural and biodegradable. A concise study performed by *Alizadeh-Sani et al*., in which CNFs along with some other additives namely

titanium dioxide (TiO_2) nanoparticles and rosemary essential oil (REO) were used. Films were prepared by casting and evaporation method, and characterized by XRD, SEM, and FTIR. The physicomechanical, barrier-analysis, antibacterial, and antioxidant capabilities of the films were examined in relation to different CNF, TiO2, and REO concentrations. Remarkable results related to water resistance, homogeneous dispersibility, increment in Tensile strength (TS) and Young Modulus were noticed [110]. *E. Fortunati et al.* prepared bionanocomposite gluten films by using CNFs and CNCs derived from sunflower stalk. Both the CNC and CNF derived cellulose nanoparticles were implanted in gluten matrix, and their impact was examined. A uniform morphology, the absence of cellulose nano-reinforcements that could be seen, and the existence of tiny holes for Gluten CNF nanocomposites were all underlined by morphological examinations. Gluten reinforced with CNC decreased the water vapors permeability coefficients, however, the gluten with CNF exhibited a larger reduction. This phenomenon could be connected to the capacity of CNCs to increase the convoluted paths of vapor (gas) molecules. Additionally, the findings from the thermal, mechanical, and barrier properties analyses supported the robust interactions between CNC and the gluten matrix attained throughout the process [111]. Another work done by *Bagheri et al*, in which physiochemical properties of bionanocomposite films made with gluten containing CNFs and carboxymethyl cellulose (CMC). Response surface methodology (RSM) was used to examine the impact of WG, CMC, and CNFs concentrations, on the mechanical, color, and water vapor permeability (WVP) characteristics of the biodegradable nanocomposites [33].

1.7.9 Gluten Films by using Modified CNFs (mCNFs)

Very little research on the bionanocomposites, reinforced with modified cellulose nanofibers that are based on gluten, has been documented. Although modified/ esterified CNFs use in different polymers is found in literature. For example, *Weijun Yang et al*. used esterified CNCs in Polyvinyl Alcohol Films (PVA), to find out thermomechanical, antioxidant and moisture behavior of the films. The results of showed that, PVA/mCNC films could be regarded as potentially high-performance active food packaging materials [112]. A study performed on the production of plastic-free bioactive paper coating, in which modified CNFs were used as reinforcing agent, showed promising results [113]. For thermoset and thermoplastic polymers like high-density polyethylene, polypropylene, polystyrene, nanocellulose--the most promising substitute nanosized filler, offers great stiffness, strength, decreased weight, thermal stability, flame retardancy, and biodegradability [114]. However, the studies of same effects on WG

nanocomposites are very rare in literature. The core of my research is to find out the effects and changes on film after using mCNFs in gluten films.

1.8 Ionic Liquids (ILs)

Cations and anion-containing liquid (aqueous) salts, in which at least one of cation/ anion is an organic radical, with melting points lower than 100 °C, are referred to as ionic liquids (ILs). The broad consensus is that they are regarded as non-volatile, non-flammable, and low vapor pressure liquids. Strong thermal stability, strong ionic conductivity, and low viscosity are only a few of their distinctive physicochemical characteristics that are well recognized [115]. There are several types of ionic liquids, and they can be classified according to the nature of their cations and anions. Some examples include.

1. Imidazolium-based Ionic Liquids
2. Pyridinium-based Ionic Liquids
3. Phosphonium-based Ionic Liquids
4. Ammonium-based Ionic Liquids

Ionic liquids are being used enormously in different applications due to their promising characteristics. Currently they are used in extraction and separation of chemicals [116], drug delivery [117], food preservation [118], electronics, environmental remediation [119], as lubricants [120], catalysts [121], and solvents for chemical synthesis [122]. They are also being used for the production as well as modification of cellulose nanofibers [123].

Figure 1.6 Possible technologies generated from the cellulose dissolved in ILs.

1.8.1 ILs and Cellulose Dissolution

In 2002, first publication on cellulose dissolution was published by *Rogers et al.* [124]. It investigated ionic liquids that combined the 1-butyl-3-methyl imidazolium cation with various anions as cellulose solvents. In comparison to big, non-coordinating anions, it was discovered that chloride, a tiny hydrogen bond acceptor, was the most efficient anion to dissolve cellulose. Since then, other ionic liquids with the capacity to effectively dissolve cellulose, have been documented in literature. Examples include those containing halide substitutes like BMIMCl and various counter anions like phosphate, formate, and acetate. The relatively high viscosities of ionic liquids containing halide anions are a drawback since they complicate processing during the dissolution. Ionic liquids containing anions, such acetate, formate, and phosphate, have lower viscosities, which makes them more useful for a variety of applications [125]. Due to its decreased viscosity and greater capacity to dissolve cellulose, 1-ethyl-3-

methylimidazolium acetate ionic liquid is now used to produce commercially accessible cellulose solutions.

1.8.2 Chemical modification of Cellulose in ILs

The one major application of cellulose dissolution in ionic liquids is their use as solvent media for transforming cellulose chemically. The use of conventional solvent systems (organic compounds) for such purposes has been constrained by their high toxicity, laborious nature, and partial recovery. Therefore, several research has been conducted to utilize ionic liquids as reaction media for the functionalization of cellulose since the advent of the successful utilization of ILs for the dissolving and modification of cellulose. There are some possible modifications by using ionic liquid as a dissolving medium, illustrated in figure 1.7.

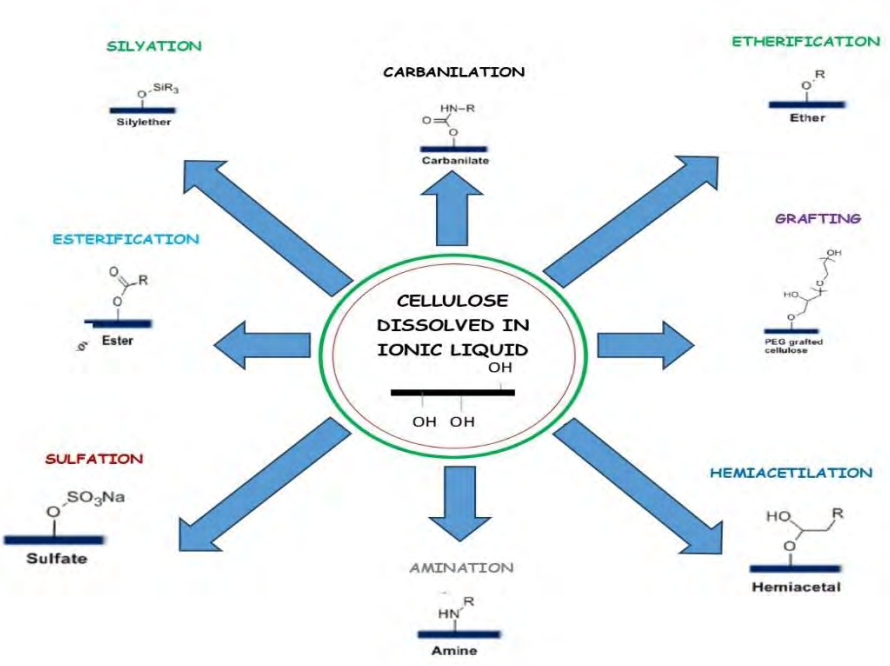

Figure 1.7 Possible chemical modifications of cellulose by using ILs as a dissolution medium

1.8.3 Cellulose Composites by using ILs

Because ionic liquids dissolve cellulose so well, they have been frequently used to make cellulose-polymer blends. To begin, both the polymer and the cellulose are dissolved in the ionic liquid. The blended polymeric mixture is then extracted from the resultant homogenous

solution, and the ionic liquid is eliminated. For instance, cellulose and natural biopolymer wool were mixed by combining them in a mutual IL solvent like 1-butyl-3-methylimidazolium chloride [126]. A composite material with more thermal stability than each of its components was produced by precipitating the solution, comprising both ingredients, in water. Additionally, when the cellulose percentage of the composite increased, its mechanical strength also increased, and the values of the composite for elongation at break were noticeably higher than those of separate components. It is also important to note that following composite manufacture, the ionic liquid solvent was recovered with great yield as well as purity. Other than being used as a solvent, the direct polymerization of ionic liquid monomers in the presence of cellulose can also yield cellulose composites. Due to their strong affinity and compatibility, imidazolium-based ionic liquid monomers offer excellent potential to interact with cellulose. Because of this, *Murakami et al.* created 1-(3-acryloyloxybutyl)-3-methylimidazolium bromide (AcMIMBr), an ionic liquid monomer of the imidazolium type [127]. In the end, the monomer and cellulose were mixed in 1-butyl-3-methylimidazolium chloride (BMIMCl), an ionic liquid, and the in-situ polymerization was performed at high temperatures with an initiator present. In our study, we used pyridinium based ionic liquid carrying halide anion. The ionic liquid was mixed with CNFs and mCNFs in the presence of glycerol and then wheat gluten was added to the mixture and mixed well to make dough for gluten films. The IL containing films may have new characteristics that could be helpful in strength and barrier properties of the films.

Aims and Objectives

The aims and objectives of the thesis are:

- Production of quality CNFs from different waste biomasses by using simple and easy chemo-mechanical methods.
- Modification of CNFs to improve their compatibility with gluten proteins and their functional properties.
- Assessment of modified CNFs in terms of structure and size.
- Composites formation by using gluten and mCNFs into thin biobased films.
- Development of specific functional properties such as antimicrobial properties, via film coating, for utilization in food packaging.

CHAPTER 2

MATERIALS AND METHODS

2.1 Chemicals

Chemicals used in this study were 98% sodium hydroxide (NaOH), 70% Nitric Acid (HNO_3), 97% sodium nitrite ($NaNO_2$), 86% potassium hydroxide (KOH), purchased from Sigma-Aldrich; 80% sodium chlorite ($NaClO_2$) and 99% Urea (CH_4N_2O) from UNI-chem; 99.9% benzene (C_6H_6) from DUKSAN; 99.9% Absolute Ethanol from RCI Labscan; 98% sulfuric acid (H_2SO_4), 35.4% hydrochloric acid (HCl), and 99.8% glacial acetic acid (CH_3COOH) were purchased from Sigma. For Modification of CNFs, 99.5% toluene ($C_6H_5CH_3$), 99% para-aminobenzoic acid (PABA), sulfuric acid, and ethanol were acquired from Sigma-Aldrich. For gluten films, 99.65% glycerol ($C_3H_8O_3$) from Sigma; industrial wheat gluten was acquired from Lantmannen AB Sweden. All reagents used in this study were analytical grade.

2.2 Reagents Preparation

Acidified Sodium Chlorite

By suspending 2.5 g of $NaClO_2$ in 14 mL of acetic acid and increasing the volume to 100 mL with deionized water, 3% w/v stock solution of acidified sodium chlorite was created. From a 3% stock solution of acidified sodium chlorite, different concentrations of sodium chlorite (0.5% and 1%) were prepared.

3% Potassium Hydroxide

3% w/v solution of KOH was prepared by dissolving 0.38 g in distilled water (dH_2O) to make a total volume of 12.5 mL of solution.

6% Potassium Hydroxide

6% w/v solution of KOH was prepared by dissolving 0.75 g of KOH in dH_2O to make a final volume of 12.5 mL.

0.2 M Nitric Acid Solution

Stock solution was prepared by dissolving 0.9 mL of HNO_3 in dH_2O and made the solution of 100 mL volume.

5% Toluene and Sulfuric Acid solution

Took 5 mL toluene and 5 mL of sulfuric acid and mixed them both with distilled water to make 100 mL solution.

2.3 Preparation of CNFs

Cellulose nanofibers were produced from waste cellulosic biomass by using 2 different methods. Both methods were chemo-mechanical and easy to perform on laboratory scale. Two sources, namely *Eucalyptus* bark (EU) and sugarcane bagasse (SCB), were used to derive CNFs. The *Eucalyptus* bark was collected from a tree in Quaid-I-Azam University Islamabad, and sugarcane bagasse was taken from a local stall of Bhara Kahu, Islamabad. Both samples were sterilized with 70% ethanol, and then air dried for 3-4 days. After drying, both samples were grounded to powder form, using a SilverCrest coffee grinder.

2.4 Method 1 (Chemical treatment; CT)

The procedure used was taken from *Kumar et al*. (2019) [128] for the extraction of CNFs from both EU as well as SCB. 1 g of both samples in the powder form were taken separately. Both samples were subjected to strong alkaline treatment by soaking in 12% w/v solution of NaOH at room temperature, for 24 h under continuous stirring. After alkaline treatment, the samples were rinsed with distilled water until they got neutralized (pH=7). Now the alkali treated samples were added with 0.2 M nitric acid solution (14 mL) and mixed well, and finally added 1.96 g of sodium nitrite and closed the flask tightly to avoid any escape of newly formed NO_2 gas. The solution thus formed was kept on hot magnetic plate for 10-12 h at 60-70 °C, and 500 rpm stirring. After HNO_3 treatment the sample was removed from hot plate, washed with distilled water, and sample solids collected on filter paper. After washing, samples were added to ethanol: water mixture in ratio 2:1 and centrifuged at 4000 rpm for 1 h. Multiple washings were performed until the pH was neutralized. Finally, the samples were poured in labeled petri plates and kept in an incubator for 2 to 3 hours at 55 °C for complete drying. The dried samples were grinded again and stored in falcon tubes (Figure 2.1).

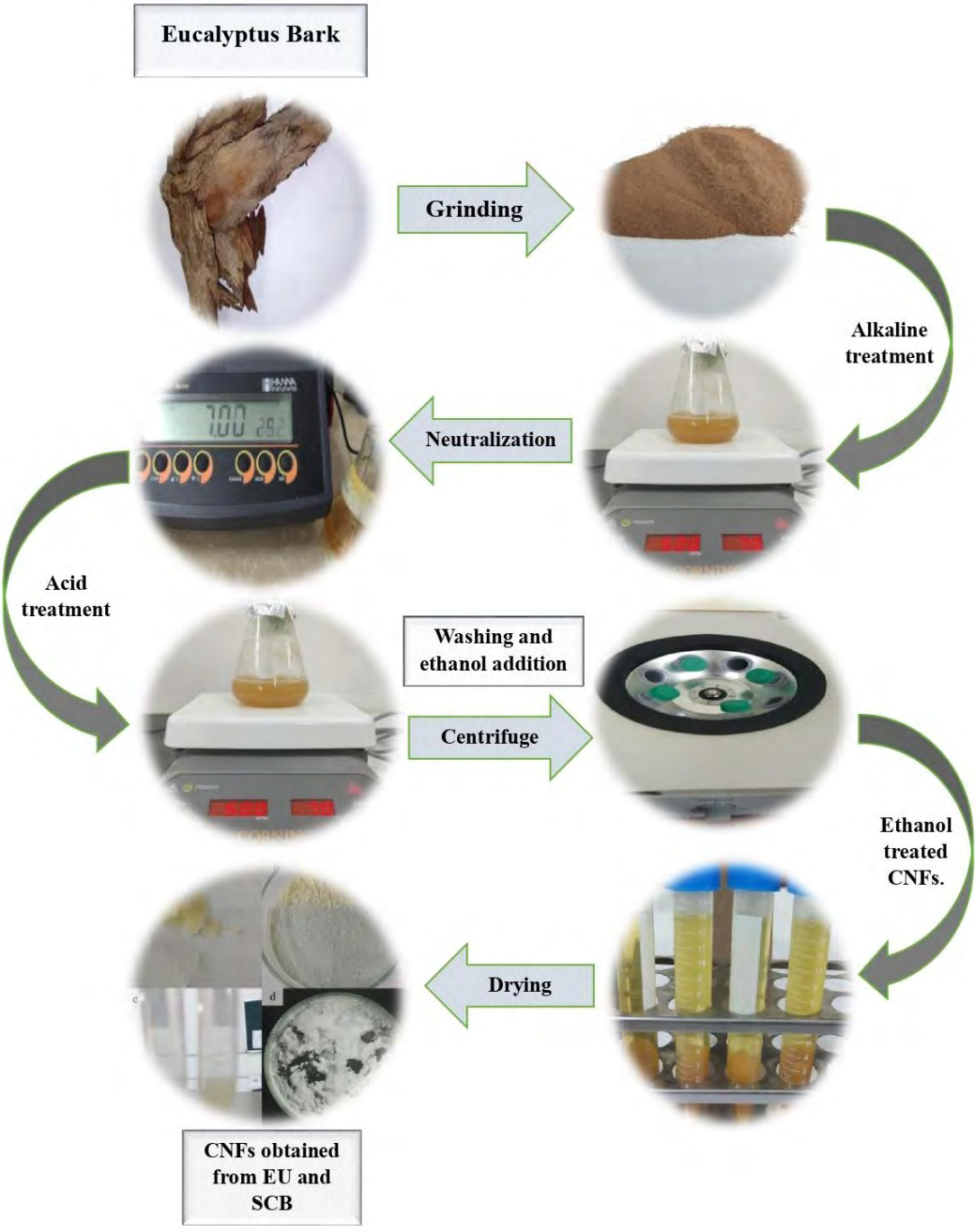

Figure 2.1 The steps by which the SCB and EU are processed and converted to CNFs.

2.5 Method 2 (Pre-treatment; PT)

In this method, the ethanol-water treated powder form sample, which was free from contaminants, was put through Soxhlet extraction. The Soxhlet extraction is used to remove wax from the sample, it weakens the bonds between cellulose, lignin and hemicellulose, and makes the cellulose isolation easy in the next steps by providing mechanical support. to remove the wax, 20 g of each sample were refluxed at 70-75 °C for 6 h with a solution of 2:1 benzene and ethanol, respectively. The process was carried out using a Soxhlet apparatus shown in the Figure 2.2.

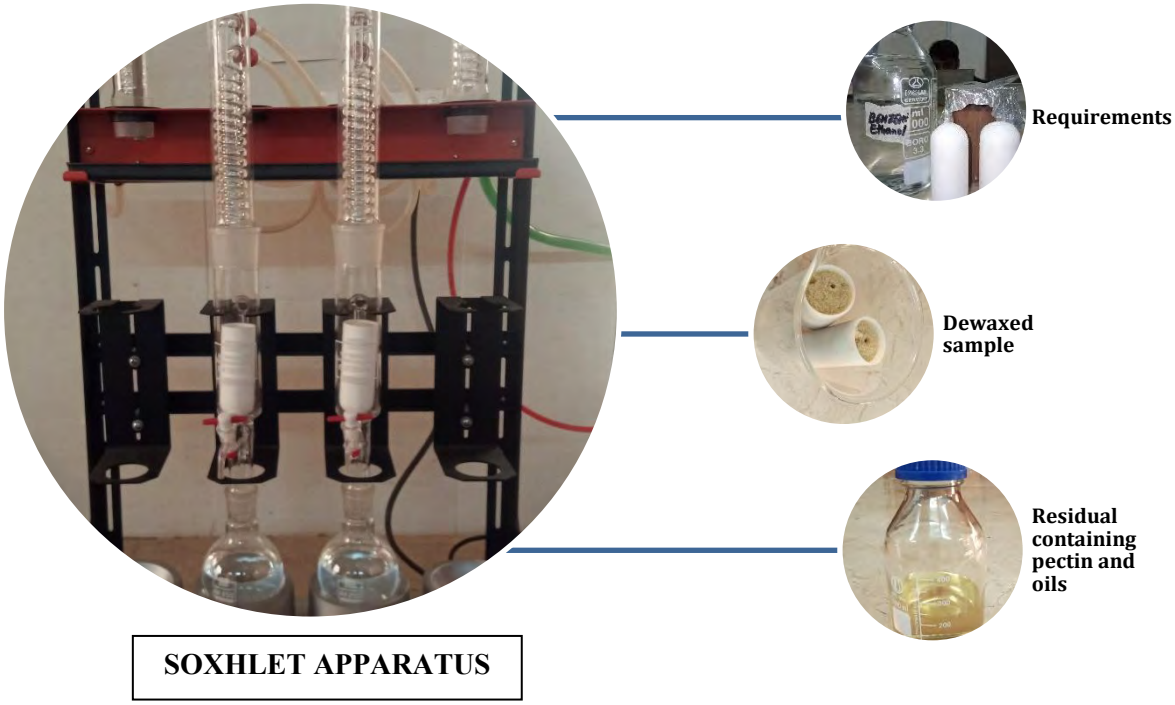

Figure 2.2 Soxhlet apparatus working on 60 °C to 70 °C for the dewaxing of sample; to weaken the bonds between cellulose, hemicellulose, and lignin.

The method 2 consists of 3 major parts after pretreatment. First is Acid hydrolysis to remove maximum lignin out of the sample; the second one is alkaline treatment to extract maximum hemicellulose out of the sample; and in the last ultrasonication of the sample to disintegrate the cellulose fibers from micro to nanoscale level.

2.5.1 Acid Hydrolysis

The lignin was extracted by dissolving sample it in acidified sodium chlorite solution at 60 °C and 500 rpm for an hour, while stirring constantly on a magnetic stirrer. For this, an acidified sodium chlorite solution was prepared by mixing 1 g of biomass of each sample with 2.5 g of sodium chlorite, acetic acid, and deionized water. The same acid hydrolysis step was repeated 5 times, each followed by thorough washing with deionized water. The fibers were filtered using Whatman filter paper no. 40 and left at 25 °C overnight.

2.5.2 Alkaline Treatment

The samples were treated and mixed with a 3% potassium hydroxide solution at 80 °C, set for two hours before being transferred to a 6% potassium hydroxide solution at 80 °C, and then set for two hours. The primary purpose of this two-phase treatment of the sample was to completely remove and leach out any hemicellulose, leftover starch, and pectin (usually present in hard wood). The impurities hemicellulose, starch and pectin were removed by filtering the solution with deionized water after each KOH treatment. The pH was neutralized by repeated washing with deionized water after each alkali treatment.

2.5.3 Ultrasonication

The chemically purified cellulose fibers, which were obtained from the two different types of plant fibers, were soaked in a container of distilled water (120 mL), and the cellulose suspensions thus obtained were then brought for ultrasonication, for 30 min using a ultrasonicator machine, to isolate the nanosized fibers of cellulose. After sonication, the sample was centrifuged at 13000 rpm for 20 min. Supernatant suspension was taken and the suspension was poured in petri plates for drying. The drying was done at 55 °C in an incubator.

2.6 Chemical Modification (Esterification) of CNFs

For modification of cellulose nanofibers microwave assisted method presented by *Farida Baraka et al.* [86] was used. In that method, the dried sample was ground to powder form by using a mortar and pestle. Three main chemicals are required for modification. Toluene prevents reacting substances from entering and interacting with the bulk sites of the fibers, hence promoting surface alteration of the fiber. Sulfuric acid acts as catalyst in the reaction. PABA or para-amino benzoic acid is the chemical which makes esterification reaction with -

OH sites on the fiber. Around 50 mg of the powder form CNF was taken into a quartz cup and 10 mL of toulene: sulfuric acid solution was added. 100 mg of PABA was added into the cup and closed it tightly to avoid any escape of toluene vapors. Tightly closed cup was treated in a microwave oven set at 80 °C for 15 minutes. After 15 minutes the sample was removed and kept at low pressure for 5 hours to evaporate the toluene completely. Then few mL of ethanol was added dropwise, with continuous stirring, to solubilize the unreacted PABA for several minutes. In the final step the solution was filtered by using a Buchner funnel and simple Whatman filter paper no. 40. Lastly, the drying process of the product was done by providing temperature of 50 °C for 48 hours and stored in airtight falcon tubes.

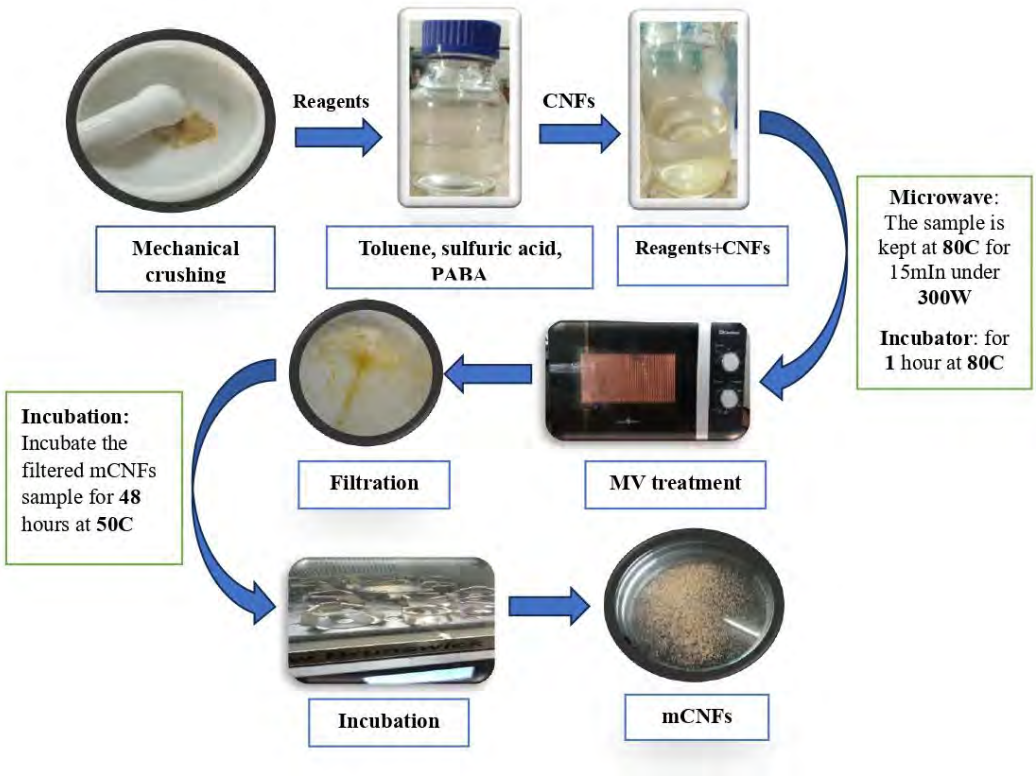

Figure 2.3 Modification Process. CNFs sample processed through both mechanical and chemical treatment followed by exposure to high temperature/radiations.

2.7 Gluten Films Formation

To prepare the gluten films containing mCNFs two hot plates working on 130 °C were required. For film making 70% gluten and 30% glycerol were used. The amount was optimized by using the same weight percentage of glycerol. In first film, 7 g (70%) gluten and 3 mL (30%) glycerol were used, which were reduced to 3.1 g and 1.9 mL respectively. 5 g films gave promising texture. Different films were prepared by using mCNFs and Ionic liquid in addition. 10 mg of mCNF was used in each film. The quantity of ionic liquid was set to 50 µL in each film. The resulting dough was kept between two hot plates working at 130 °C and manual pressure at a rate of 100 kg/m^2 was applied to compression mold into a thin film.

Table 2.1 Summaries of the wheat gluten films and their abbreviations.

Wheat gluten films	**Abbreviations**	**Label**
Wheat gluten and Glycerol	WG-Gly	Film 1 (Fig 2.4)
Wheat gluten, Glycerol and CNFs	WG-Gly-CNFs	Film 2 (Fig 2.5)
Wheat gluten, Glycerol, CNFs, and Ionic Liquid	WG-Gly-ILCNFs	Film 3 (Fig 2.6)
Wheat gluten, Glycerol, mCNFs	WG-Gly-mCNFs	Film 4 (Fig 2.7)
Wheat gluten, Glycerol, mCNFs and Ionic Liquid	WG-Gly-ILmCNFs	Film 5 (Fig 2.8)

2.7.1 Chitosan and Salicylic Acid Coating

In this experimental procedure, 1 g of chitosan was dissolved in 25 mL solution of dilute acetic acid and subjected to continuous stirring on a hot plate at 60 °C until a clear solution was obtained. Simultaneously, 1 g of salicylic acid was dissolved in 25 mL of ethanol and placed in an orbital shaker, set to 100 rpm, to facilitate complete dissolution. Subsequently, the two solutions were combined, and the resulting mixture was subjected to continuous stirring on a hot plate to achieve a homogenous solution. This process led to the formation of a thick, concentrated solution. To apply the solution as a coating, a fine brush was used to coat films [129] .This method ensured the uniform distribution of chitosan and salicylic acid in the solution, allowing for a controlled and consistent application of the coating on the films.

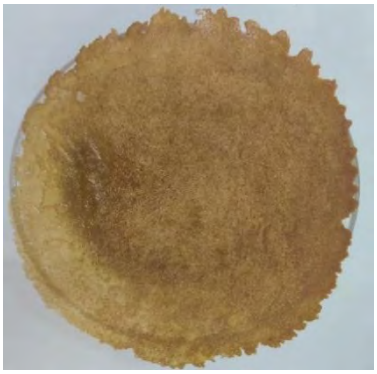

Figure 2.4 WG-GLY

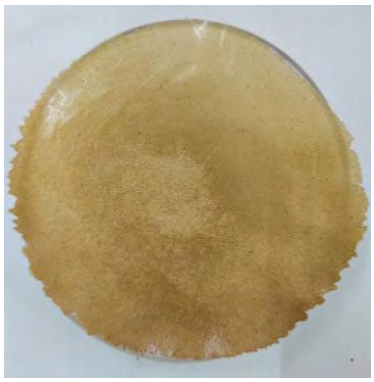

Figure 2.5 WG-GLY-CNFs

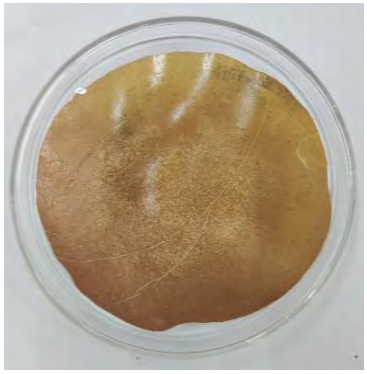

Figure 2.6 WG-GLY ILCNFs

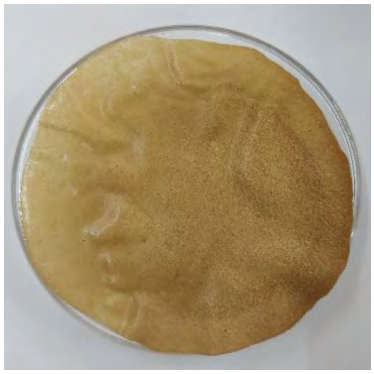

Figure 2.7 WG-GLY-mCNFs

Fig 2.8 WG-Gly-ILmCNFs

CHARACTERIZATION

2.8 Characterization of CNFs and mCNFs

To find out the success of extraction and modification, the samples were characterized by following analytical approaches:

2.8.1 FTIR spectroscopy

The basic principle of FTIR spectroscopy is that when infrared radiations are absorbed into the molecule, they increase the vibrational modes inside the molecule. These vibrational modes refer to the ways in which the atoms of molecule can vibrate relative to each other. The frequencies of these vibrations are determined by the potency of the bonds among the atoms of a given molecule along with the mass of the atoms. The different functional groups in the cellulose sample were identified using FTIR spectroscopy and their vibrational characteristics. The tool was used to capture the FTIR spectra of the sample. This FTIR instrument had a 400–4000 cm^{-1} wavenumber range of IR radiation. The sample was used in the powder form for this analysis. This powder may be converted to fine powder form by using fiber microtome. In fine grinding, KBr (Potassium Bromide) is used to obtain full transmittance of the spectra because KBr shows 100% transmittance between 400-4000cm^{-1} range. When the sample is kept into the machine the infrared radiations pass through the sample, the number of radiations that are absorbed at different wavelengths by the sample are noted and show in the form of absorption spectrum. This absorption spectrum is the unique fingerprint of exact molecular structure of the sample. This spectrum is used to identify the sample as well as its chemical composition. FTIR spectroscopy is non-destructive, fast, easy, and highly sensitive in its action. It can be used to analyze a vast variety of materials.

2.8.2 Zeta-potential and particle size analysis

The nanofibers samples obtained from sugarcane bagasse SCB and Eucalyptus EU were characterized by using laser diffraction apparatus (Malvern Instruments Ltd., Mastersizer 2000—model APA2000, UK). It is a versatile machine, used to measure the size distribution of vast range of particles from micrometers to very small nano scale. It is very precise instrument with uncertainty rate of ±1%. It can be used for a variety of samples like liquids, suspensions, and powders. This machine is easy to handle and employed with a dispersion unit

(Hydro 2000S, model AWA2001) which elevates and enhances the dispersibility of the sample to give better results. Water is a suitable solvent for sample immersion. Zeta sizer cells are used to load the samples. The samples are added with the help of syringe into the cells with tight and fixed conformation to avoid any bubble formation into the cells. After loading, the cells are kept into the holders of zeta sizer machine one by one. After loading the cells into the machine, the particles present in the sample are dispersed using high frequency acoustic waves. The zeta potential of each particle influences how it travels, and the high frequency causes the particles to flow randomly in the liquid. A laser beam is passed through the disperse sample in the next step. This beam causes the scattering when passed through the sample and is collected by a detector (Malvern Instruments Ltd. Zeta sizer Nano series —model Nano ZS, UK). This detector counted the amount of scattered light and interpreted the dimensions of CNFs sample i.e., the surface charge and length of the fibers. Two CNFs samples and two mCNFs samples were tested in zeta sizer machine to check the differences occurring before and after the modification of samples; the changes related to size and charge occurred after the modification of samples.

2.8.3 UV-Vis Spectroscopy

An analytical technique that offers qualitative and quantitative examination of organic and inorganic chemicals in the field of chemical research is known as UV-Vis spectroscopy. This technique has a wide range of applications and is typically used to determine chemicals in extremely tiny concentrations. Depending upon the state of electrons found in the analyzed molecule, electron excitation that takes place in UV-Vis spectroscopy, is captured in the form of a spectrum represented as wavelength and absorbance. The wavelength that is absorbed, increases with the ease of electron excitation, and the absorbance increases with the number of excited electrons. The sample can be of any form liquid, gas, or vapor, to be identified using UV-Vis spectroscopy. The transformation of sample into a transparent solution is required. The dissolution of the sample in the form of a solution is needed, the solvent employed must be devoid of conjugated double bonds and colorless, there is no interaction with the molecules of the substance being analyzed, and the solvent has high purity.

2.9 Characterization of Composites

2.9.1 FTIR Spectroscopy

FTIR Spectroscopy was performed to identify the molecular interactions between the nanofibers and wheat gluten proteins. These protein-cellulose interactions may improve the mechanical properties of composites along with other beneficial results like the barrier property of composites against factors such as oxygen and moisture.

2.9.2 Solubility Testing

A process used to find out the extent to which a substance is dissolved in a particular solvent under specific conditions i.e., temperature and pressure. All the gluten composites films including control, mCNFs inserted, and CNFs inserted, were dissolved in water and nitrous acid solution for 24 h under continuous stirring, to find out the percentage dissolution of samples.

2.9.3 Antimicrobial Assay

The CNFs modified by esterification using PABA were used in the gluten films. These gluten films containing CNFs, mCNFs, ionic liquids and chitosan-coated, were treated with different bacterial strains to check their antimicrobial activity. The thin small sections of films were exposed against the strains *K. pneumonia*, *P. aeruginosa* and *Bacillus subtilis***.**

CHAPTER 3

RESULTS

3.1 Fourier transformed infrared spectroscopy (FTIR)

EU-CT Eucalyptus CNFs sample

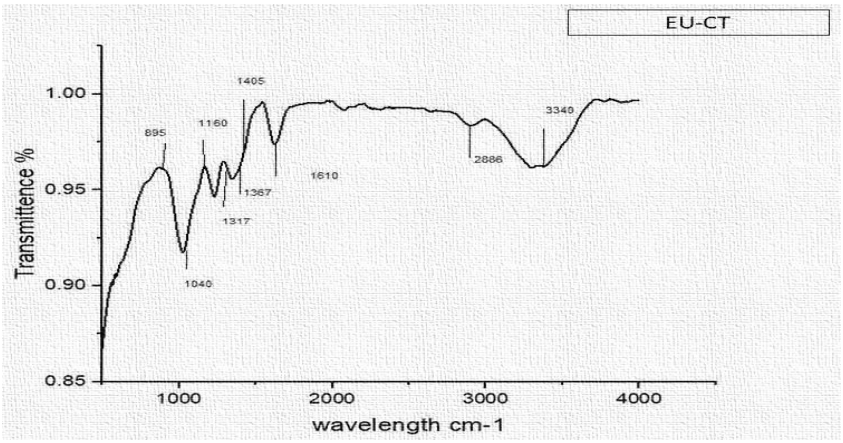

Figure 3.1 FTIR-spectrum of CNFs extracted from eucalyptus bark by using chemical treatment (CT)

EU-CT modified CNFs sample

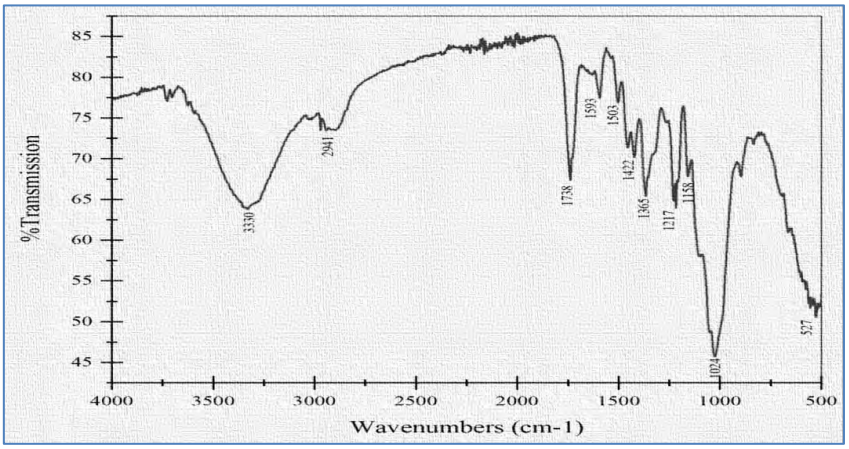

Figure 3.2 FTIR-spectrum of esterified EU-CT mCNFs

SCB-CT simple CNFs from Sugarcane Bagasse

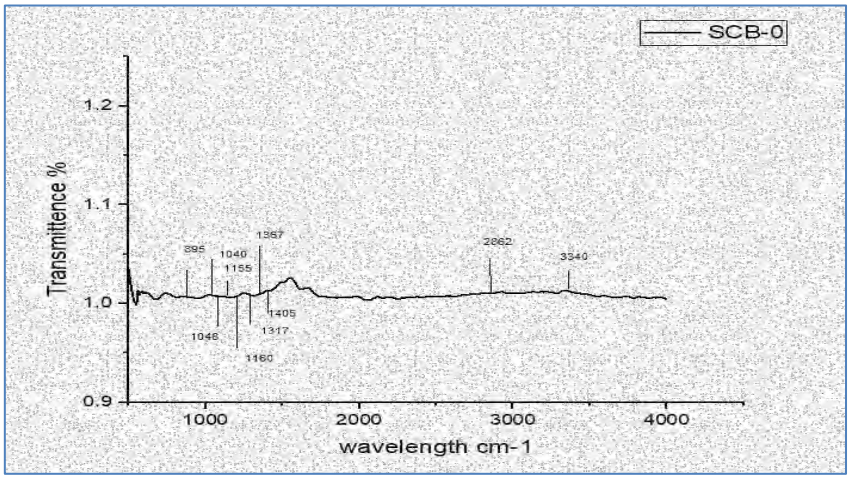

Figure 3.3 FTIR-spectrum of CNFs obtained from SCB-CT

SCB-CT modified CNF sample

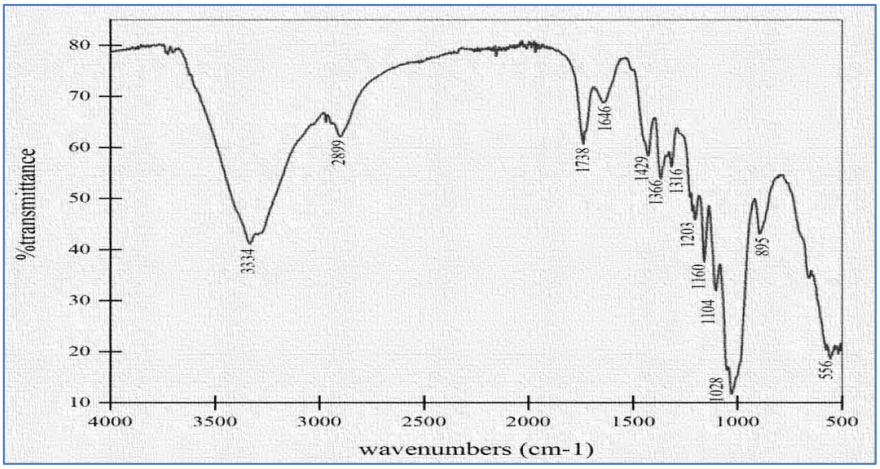

Figure 3.4 FTIR-spectrum of SCB-CT mCNFs sample

Table 3.1 IR spectrum chart of different frequencies observed in the FTIR analysis of nanofibers samples [130].

ABSORPTION (cm^{-1})	GROUPS/ STRETCHING
500-600	C-X Halogen stretching
1025-1030	C=O Carbonyl group stretching
1030-1250	C-N medium stretching
1335-1370	S=O strong stretching
1395-1440	Medium O-H bending
1566-1640	Cyclic alkene C=C stretching
1735-1750	Esterification C=O stretching
2700-3200	O-H and N-H stretching
3200-3350	Intramolecular O-H stretching

3.2 Particle size distribution and Zeta potential analysis

The zeta potential and particles size in a liquid media are measured using a zetasizer, which is a particle size analyzer that operates on the dynamic light scattering (DLS) concept. The Brownian motion of particles, characterized by their arbitrary movement brought on by the collisions with nearby molecules, is measured using DLS. The Brownian motion of the particles increases with their size.

3.2.1 Comparison of Zetasizer analysis of CNFs and mCNFs from EU and SCB

Here are some results of size (nm) and potentials (mV) of modified as well as unmodified cellulose nanofibers samples.

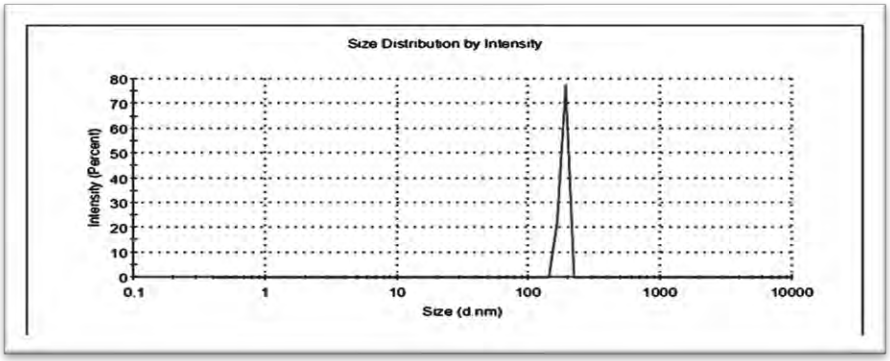

Figure 3.5 PSD of EU-CT CNFs.

The size of the nanofibers obtained from Eucalyptus sample was around **184 nm** according to the data obtained from zetasizer analysis.

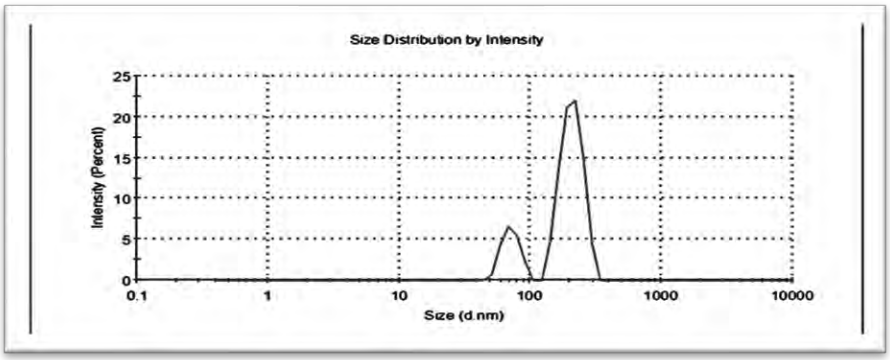

Figure 3.6 PSD of EU-CT mCNFs. Two bimodal peaks appeared at **71.23 nm** and **208.7 nm** appeared after modifying the sample by 4-paraamino benzoic acid.

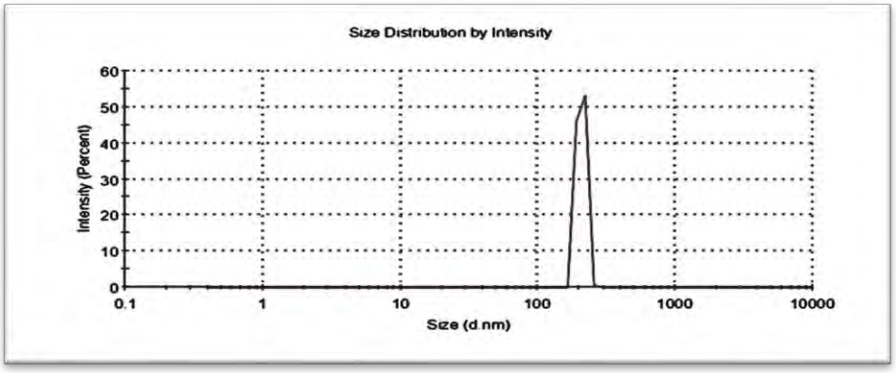

Figure 3.7 PSD of SCB-CT CNFs.

The value of size distribution obtained from Sugarcane bagasse CNFs was **208 nm**.

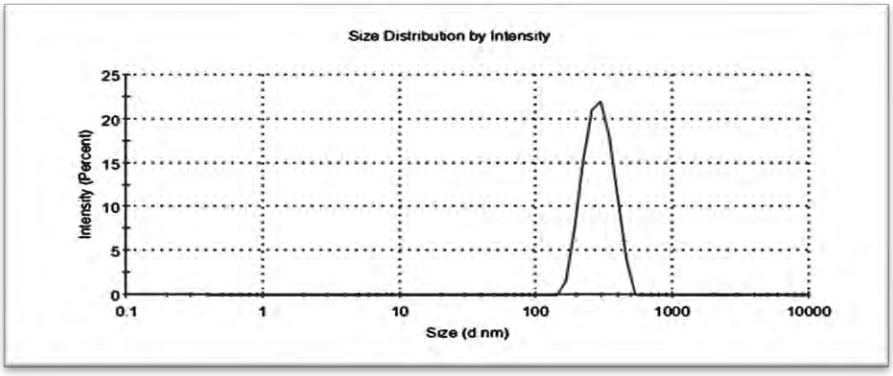

Figure 3.8 PSD of SCB-CT mCNFs

The size of modified CNFs from SCB changed from **208 nm** to **290 nm**.

4.2.2 Zeta potential analysis of CNFs and mCNFs from EU and SCB

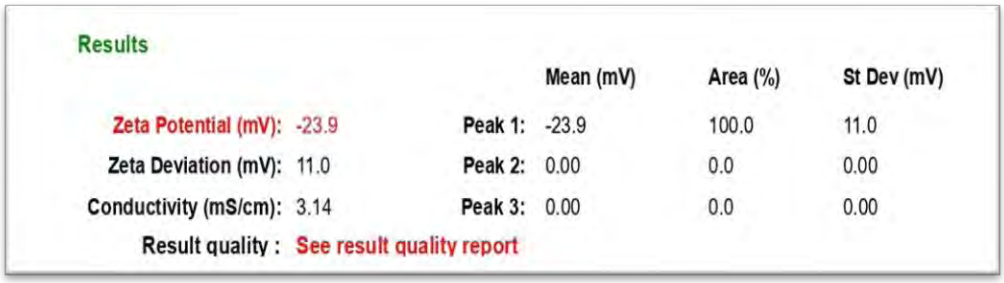

Figure 3.9 Zeta potential obtained from EU-CT CNFs.

The potential of EU fiber was calculated by the zetasizer was around **-23.9 mV** with the conductivity **3.14** $\boldsymbol{mS/cm}$

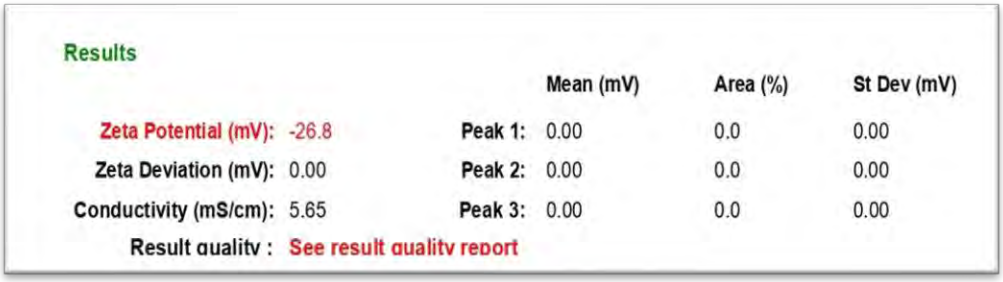

Results

		Mean (mV)	Area (%)	St Dev (mV)
Zeta Potential (mV): -26.8	Peak 1:	0.00	0.0	0.00
Zeta Deviation (mV): 0.00	Peak 2:	0.00	0.0	0.00
Conductivity (mS/cm): 5.65	Peak 3:	0.00	0.0	0.00

Result quality : See result quality report

Figure 3.10 zeta-potential obtained from EU-CT mCNFs.

The potential modified EU fibers calculated by the zetasizer was equal to **-26 mV** with the enhancement in the conductivity raised to **5.65 mS/cm.**

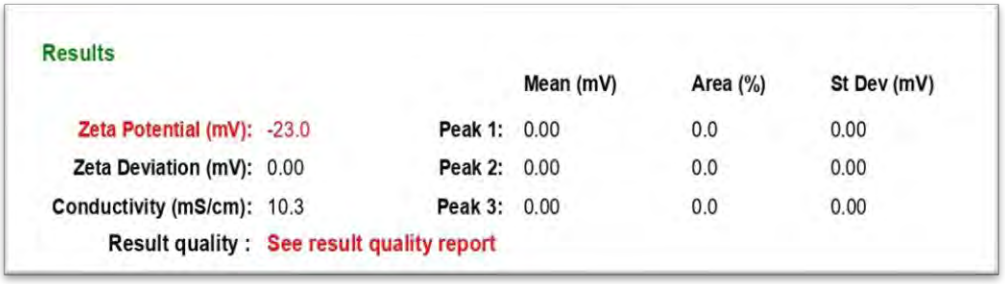

Results

		Mean (mV)	Area (%)	St Dev (mV)
Zeta Potential (mV): -23.0	Peak 1:	0.00	0.0	0.00
Zeta Deviation (mV): 0.00	Peak 2:	0.00	0.0	0.00
Conductivity (mS/cm): 10.3	Peak 3:	0.00	0.0	0.00

Result quality : See result quality report

Figure 3.11 Zeta-potential of SCB-CT CNFs.

The potential of SCB nanofibers recorded by the zetasizer analyzer was **-23 mV** with conductivity of **10.3 mS/cm.**

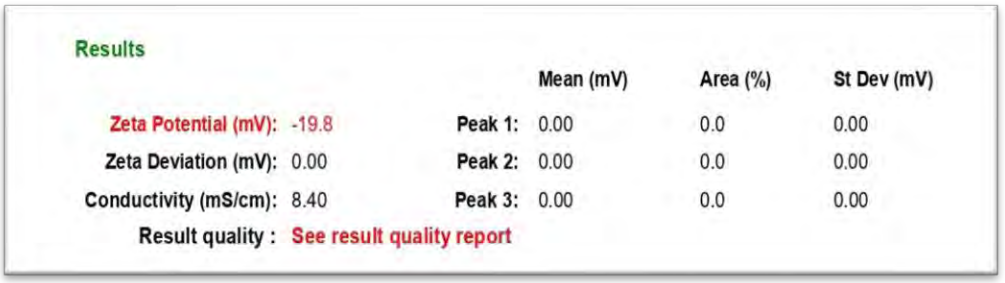

Results

		Mean (mV)	Area (%)	St Dev (mV)
Zeta Potential (mV): -19.8	Peak 1:	0.00	0.0	0.00
Zeta Deviation (mV): 0.00	Peak 2:	0.00	0.0	0.00
Conductivity (mS/cm): 8.40	Peak 3:	0.00	0.0	0.00

Result quality : See result quality report

Figure 3.12 Zeta-potential of SCB-CT mCNFs.

The potential of SCB nanofibers after modification reduced to **-19.8 mV** and conductivity also lowered down to **8.40 mS/cm.**

Table 3.2 Particle size distribution and Zeta-potential of CNFs

CNF samples	Zeta-size diameter **(d.nm)**	Zeta-Potential (mV)	Dispersibility **PDI**	Standard deviation **%**
EU-CT	184	-23.9	1.00	10.87
SCB-CT	206	-23.0	1.00	15.60

Table 3.3 Particle size distribution and Zeta-potential of mCNFs

mCNFs samples	Zeta-size diameter **(d.nm)**	Zeta-Potential (mV)	Dispersibility **PDI**	Standard deviation **%**
B EU-CT	71.23, 208.7	-26.8	0.665	10.83, 39.19
C EU-CT	290.8	-19.8	0.224	69.41

3.3 UV spectroscopy

To check out the success of esterification UV/Vis Spectroscopy was performed. The solvent used to solubilize mCNFs was the mixture of Urea, NaOH and water. Native CNFs were shown to absorb relatively little UV light. On the other hand, PABA showed good UV absorption between 250 and 340 nm. The UV absorbance of the CNFs with grafted PABA was equivalent to PABA UV absorbance in the 250–330 nm range[131] .

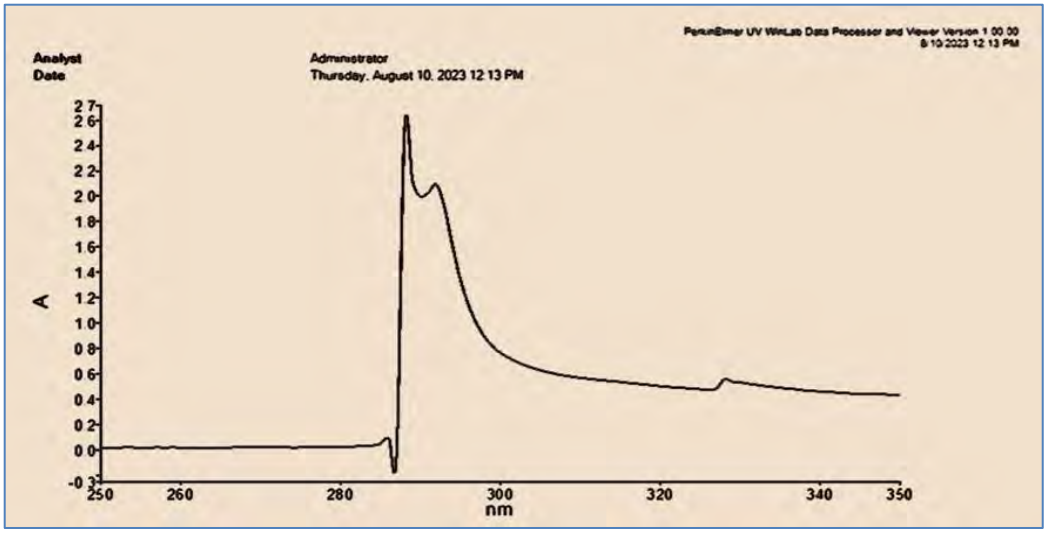

Figure 3.13 UV absorbance of modified EU CNFs.

Absorbance value of **2.6377 a.u.** with wavelength (λ) of **288.15 nm.**

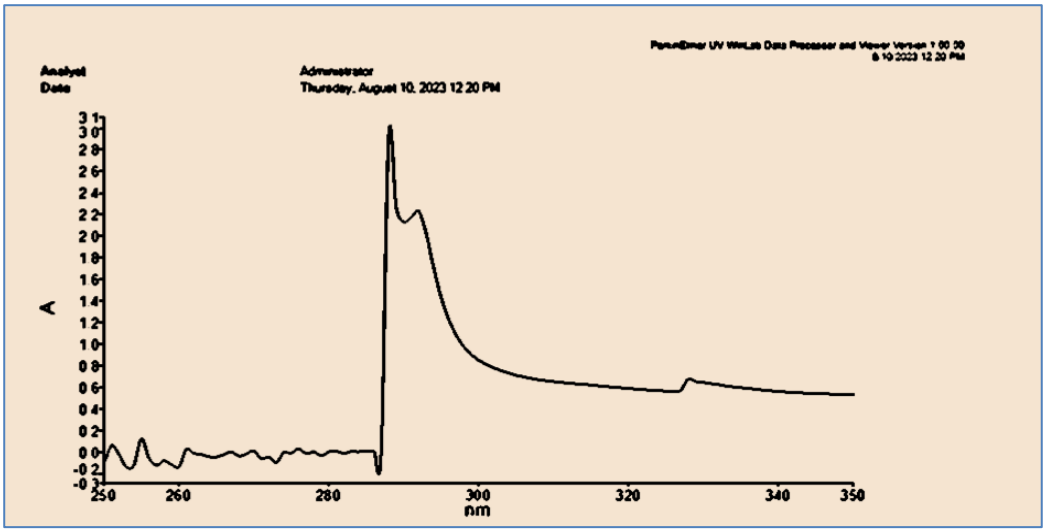

Figure 3.14 UV absorbance of modified SCB CNFs.

Absorbance value of **3.0205 a.u.** with wavelength (λ) of **288.15 nm**.

Table 3.4 Typical absorption of some common chromophores [132]**.**

Chromophores / Compounds	**λ max (nm)**
Carbonyl	186-280
Benzene	204
Toluene	207
4-Aminobenzoic acid	280-350
Urea	Below 200
NaOH	304

3.4 CNFs Composites (Gluten Films) Testing

FTIR was performed to test the integration of CNFs and mCNFs into the WG, this interaction might be helpful to increase the mechanical strength of the films. Antimicrobial property of the films was also tested to check out their sustainability and feasibility for food preservation.

3.4.1 Fourier-Transform Infrared Spectroscopy

Table 3.5 The films used for FTIR analysis.

Film	**Composition**
Film A (Control)	WG+Gly
Film C	WG+Gly+CNFs
Film D	WG+GLY+mCNF

Absorbance Peaks of FTIR

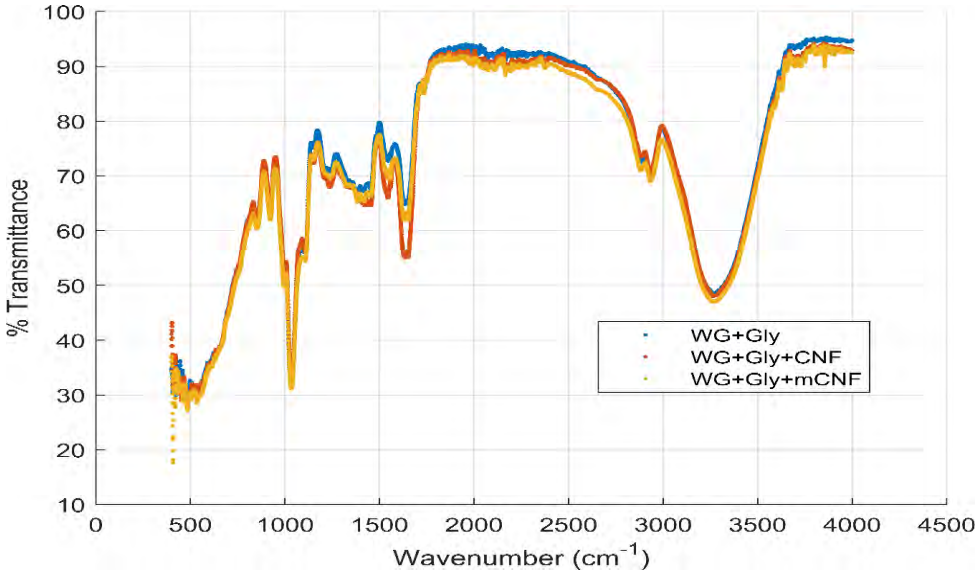

Figure 3.15 Comparative FTIR peaks of Film A, C and D.

3.4.2 Solubility Testing

Water solubility of the films was determined based on the method used by *M. Mohammadi et al.* [133]. The films were cut down into 1 cm × 1 cm dimensions. Then the films were heat dried for 48 h in a hot air incubator to remove all moisture content. Then the films were immersed in 50 mL of distilled water containing 0.2 mol of Nitrous acid (to prevent microorganism growth) for 24 h, on a magnetic stirrer. The films were then dried at filter paper and kept in a drying oven at 100 °C for 2 h. Then undissolved dried films were weighted. By reducing this final weight from the initial weight, the dissolved matter and its percentage can be calculated.

Table 3.6 Wheat gluten composites measurement for solubility test

Film No.	Composition	Initial weight (mg)	Final weight (mg)	Net Solubility IW-FW	Dissolution Percentage %
Film 1	WG+GLY	37	25.6	11.4	30.8
Film 2	WG+GLY+mCNF	29.6	20.9	8.7	29.3
Film 3	WG+GLY+CNFs	50.9	34.3	16.6	32.61

Before solubility

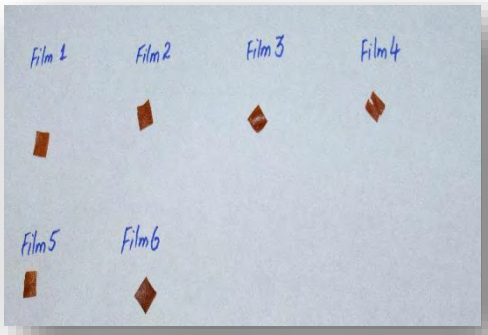

Figure 3.16

After Solubility

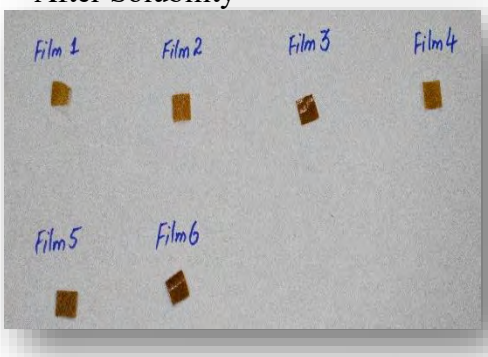

Figure 3.17

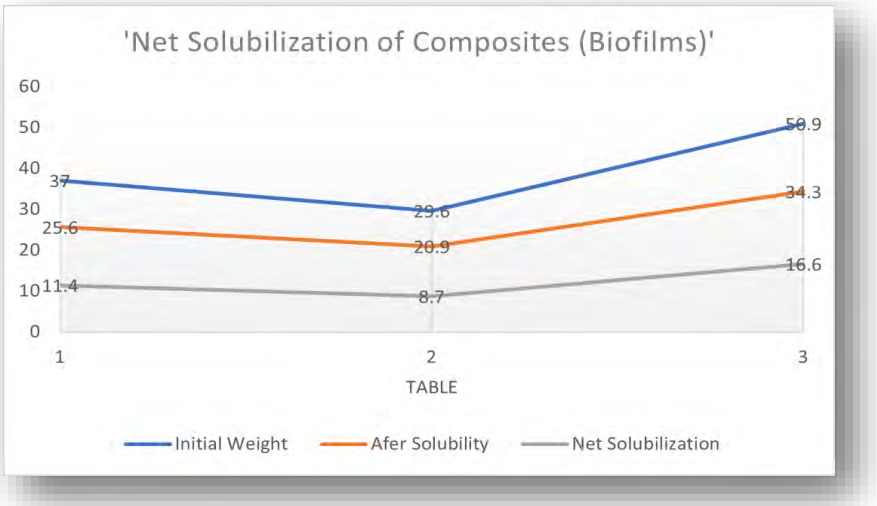

Figure 3.18 Graph showing the comparative peaks initial, final, and net solubilization of WG film composites

3.4.3 Anti-microbial Assay

Figure 3.19 Antimicrobial activity against (A) *E. coli,* (B) *S. Aureus,* (C) *S. enterica* and the control drug (D) chloramphenicol. Sample 1: WG-Gly; 2: WG-GLY-mCNFs; 3: WG-GLY-CNFs.

Samples	*Escherichia coli*	*Staphylococcus aureus*	*Salmonella enterica*
Drug (Chloramphenicol)	21	25.23	22.38
WG-Gly	9.22	14.23	17.65
WG-GLY-mCNFs	8	24.24	16.8
WG-GLY-CNFs	10.1	18	9.18

Table 3.7 Comparative values of Inhibition zones generated in result of chitosan and salicylic acid with reference to control drug (Chloramphenicol**)**

CHAPTER 4

DISCUSSION

Structural changes, as seen in the final graphs of FTIR, were brought by chemical treatment applied during the whole procedure start, from the production to modification. These changes may help in the modification of cellulose nanofibers. Moreover, the addition of 4-paraaminobenzoic acid in the modification step caused the esterification of cellulose sample at [O-H] sites. The broad peak in FTIR-spectrum of EU-CT at 3330 cm^{-1} clearly shows that the number of [O-H] groups is replacing with ester bonds [86]. In both CNFs samples, there is no peak between 1730-1740 cm^{-1}. The sharp peaks in both mCNFs samples at 1738 cm^{-1} indicate the new rising group, which identifies the ester linkage in the sample [134] . There are some other peaks that are found in FTIR-spectrum, indicating the addition or presence of different side groups which can improve the mechanical strength and the compatibility of cellulose sample. For example, [C-N] and [N-H] stretching at 1217 cm^{-1} and 2941 cm^{-1}, respectively, indicate the amino groups attached to the benzene ring of PABA, which may now be on the surface of cellulose fibers. The peaks from 3200-3350 cm^{-1} [135] indicate the medium intermolecular [O-H] stretching in the cellulose structure that shows that these bonds are connected to some other molecule which may be PABA molecules. The peak at 1028 cm^{-1} also provides the evidence of carbonyl groups [C=O] in the sample. Two similar peaks at 1158 cm^{-1} and 1159 cm^{-1} show the presence of [C-C] ring stretching which also justifies the 6-C ring of benzene present in PABA. [C-X] halogen stretching is observed in both modified samples, which may be due to addition of NaClO during the bleaching process of CNFs. The small vibrations peaks between 2000 cm^{-1} and 2500 cm^{-1} in the FTIR-spectra of both modified samples show the double bonds stretching in the molecule. The double bond stretching may be related to [C=C] or [C=N] stretching within the molecule [130].

Using the Malvern Zeta Sizer, a particle size analyzer, the PSD, and zeta potentials of CNFs and mCNFs were determined. Dispersibility (PDI) and standard deviations (S.D.) before and after the modification were also noted. In case of *Eucalyptus*, CNFs showed the diameter of about 184 nm with PDI value of 1.00 and S.D. of 10.87%. On the other hand, mCNFs, showed bimodal peaks at 71.23 and 208.7 nm, respectively, with a PDI value of 0.665 and S.D. of 10.83% and 39.19%, respectively, relative to two peaks. Bimodal peaks demonstrate the higher aggregation susceptibility of mCNFs. There is a clear shift of diameter from 184 nm to 208 nm

which indicates the addition of some bulky side group on the surface of nanofibers (PABA-esterified). The polydispersity index (PDI) shows the width of zeta size distribution; either it is totally monodispersed (PDI=0) or polydisperse. Addition of some hydrophobic group e-g PABA on the cellulose surface effectively breaks the hydrogen bonds between the fibers and make them stable and separated [17]. If the PDI value is zero, that means all the fibers in the sample are of same size. In case of CNFs, the value of PDI is 1.00, which indicates the sample is highly polydisperse. After modification, astonishingly, the value reduced to 0.665, which promised the stability of sample by making sample less polydisperse (more uniformity in dispersion). Less polydispersity causes more stability of the sample [4]. Moreover, the standard deviation shifted from 10.87 to 39.19, which means that more size heterogeneity occurred after the modification. The possible reason behind this change might be the modification percentage of sample. Not all the fibers inside the sample can get esterified in a single reaction. In case of SCB, modification caused the size increase from 206 to 290.8. Standard deviation percentage increased and PDI value reduced to 0.224. The PDI value of modified SCB was lower than modified EU. Which means the SCB fibers showed more stability after modification. The sharp peaks in SCB and EU CNFs show that they are more likely to produce shorter nanofibers.

The zeta potential, which is an indication of colloidal suspension stability, measures the degree of repulsion between neighboring, identically charged particles in a dispersion. A high zeta potential indicates stability for molecules and tiny enough particles, which means that the solution or dispersion will not coagulate. All the nanofiber suspensions in neutral water had a negative zeta potential. Similar values (-16.41 mV to -41.32 mV) have been observed for cellulose nanofibers recovered from plant waste [136]. More negative value means more electrostatic repulsion between the fibers. In case of EU-CT, the potential changed from -23.9 mV to -26.8 mV. This change of potential shows that there is an increase in the electrostatic repulsion between the fibers and enhancement in the colloidal suspension (less clumps formation). In case of SCB, the potential value decreased down to -19.8 from -20. In this case, it might be that the higher diameter increases the risk of clumps formation [137].

In both UV/Vis spectrums, the wavelength is same, which proves the addition of similar chromophore in the cellulose structure. The chromophore attached is 4-Aminobenzoic acid (PABA), the sharp peak at **288 nm** as mentioned by *Panchal et al.* [131]. The absorbance value for both samples vary. In case of EU mCNFs the absorbance value is 2.6377 a.u., which indicates that number of esterified fibers are lower than SCB mCNFs (3.0205 a.u.). So, this difference of absorbance depicts the rate of esterification of fibers. SCB fibers show more

tendency towards modification as compared to EU NFs. As shown in Zeta-sizer results, the SCB fibers are of larger size than EU fibers. Larger the size of the fiber, more of the [-OH] sites available for esterification. Sharpness of the peaks shows the interaction between PABA and cellulose nanofibers. Sharper peak means more ordered interaction between PABA and cellulose fiber. If the temperature is raised, the peak shifts to longer wavelength because the higher temperature makes PABA chromophore more disordered. Sharp peaks show the stability of modified CNFs.

FTIR graphs of the films give insights about the functional groups, chemical interactions, compatibility, and structural changes. The positive changes may improve the mechanical properties of our films and comparative analysis of modified and unmodified composites can deduce significant implications. According to the FTIR data, almost all films shared the same functional groups peaks with slight change of values. In other words, the intensities of peaks changed due to addition of NFs. CNFs shared many functional groups with wheat gluten, so FTIR graphs showed relative peaks with the difference in intensities with few new peaks. In the above films the amount of CNFs used was relatively very low--in micrograms (10-50 μg), therefore, in comparative peak analysis there is a minor difference noted. But overall, the results showed successful chemical interaction between film components. In wheat gluten essential amino acids like lysine, threonine and methionine are missing but on the other hand cysteine, proline and glutamine are found in excess along with other amino acids. In above results, the influence of gluten protein is higher due its major part in film, most of the CNFs peaks overlapped or fused with WG peaks. For example, the peaks between 3260 cm^{-1} to 3270 cm^{-1} in all graphs showed [O-H] stretching, which is common in both WG and CNFs. The peaks between 2800 cm^{-1} to 3000 cm^{-1} depict the [C-H] stretching of alkanes or aldehydes present in the sample. Alkane like region is present in both cellulose and wheat gluten and stretches are common in all graphs with slight change in the values. Glycerol also has [C-H] stretching vibrations and [O-H] stretches common with Nanofibers and WG. Amide bands are key markers of proteins. For example, Amide I band exists between 1600 cm^{-1} to 1700 cm^{-1} that shows the [C=O] groups, these are the common groups present in both CNFs and WG [138]. In case of WG film A, the value of peak is at 1633 cm^{-1} which slightly enhanced to 1637 cm^{-1} after the addition of nanofibers. [C=O] groups are the key marker of acetyl/carbonyl groups present in protein, cellulose and PABA modified cellulose. Amide II bands peaks of proteins at 1500 cm^{-1} to 1550 cm^{-1} showed [N-H] bending and [C-N] stretching. After addition of nanofibers, the intensities of the peaks became lower from 2549 cm^{-1} (WG) to 1546 cm^{-1}

due to interaction with incoming fibers. Amide III bands show [C-N] stretch, [N-H] bending, [C-H] stretch between 1200 cm^{-1} to 1300 cm^{-1}, all above graphs have values between these regions, slight changes in values showed interaction of CNFs with WG proteins [139]. A short absorbance peak is noticed in WG control film in 1700-1750 cm^{-1} region which showed aromatic [C-H] stretches of tyrosine and phenylalanine. When fused and heated with NFs, this short peak became less intense, which suggests that this might be the effect of high temperature on or fusion between two component aromatic rings of WG protein and PABA. Cellulose has fingerprint region from 600 cm^{-1} to 1400 cm^{-1} in which most functional groups are like those of proteins, after interaction with NFs slight changes in absorbance peaks were noticed. Both CNFs and WG homogenized themselves by showing strong interactions, which showed that there is strong compatibility between these two components, which favors their valuable applications in the future.

The results of solubility suggest that in WG composites containing modified cellulose nanofibers (mCNFs) the least solubility was observed, as proved by FTIR analysis the [O-H] functional groups of CNFs, which are hydrophilic in nature, are replaced by 4-aminobenzoic acid (a hydrophobic group). The addition of PABA made CNFs more hydrophobic in nature, and hence, least water solubility was observed. On the other hand, 32.61% dissolution was observed in CNF containing film. The [O-H] groups present in film might increase the solubility of films.

The produced films exhibited antibacterial properties, owing to the presence of salicylic acid. Salicylic acid is believed to harm the bacterial cell membrane, resulting in cell components leakage. Additionally, it alters the pH gradient between the cell membrane and various organelle membranes, causing a depletion of cellular energy and ultimately leading to cell death [140]. The increased antimicrobial effectiveness could be elucidated by the interaction between the amino and hydroxyl groups of wheat gluten and salicylic acid, forming intermolecular hydroxyl [C-O···H-O] and amino [N···H-O] hydrogen bonds. Comparable findings have been reported, concerning the creation of microcapsules through the combination of chitosan and salicylic acid [112]. All the films after coating with chitosan and salicylic acid showed anti-microbial properties. WG-GLY-mCNFs showed maximum inhibition zone 25.24 cm against *S. aureus* strain. Food-borne pathogens, namely *E. coli*, *S aureus*, and *Salmonella enterica* strains were tested for and a clear zone of inhibition was visible against each strain.

Conclusion

Cellulose is a remarkable biopolymer, ubiquitous on Earth and possesses exceptional nanoscale attributes, such as heightened tensile strength, elasticity, piezoelectricity, and surface reactivity. CNFs were synthesized by two different easy and economical, chemo-mechanical methods from two different biomasses including eucalyptus bark and sugarcane bagasse. Leveraging para-aminobenzoic acid surface esterification, cellulose nanofibers (CNFs) exhibited super hydrophobicity, making them prime candidates for eco-friendly biocomposite. Integration of these value-added nanofibers into wheat gluten further enhanced the strength and porosity of composites. Characterization studies affirmed the successful extraction of CNFs; zeta-size analysis attesting to their nanoscale dimensions and excellent dispersion; and FTIR analysis confirmed all the functional groups present in the cellulose nanofibers. Chemical modifications were evidenced by FTIR, Zeta-potential and UV-Vis spectroscopy, confirming the integration of para-aminobenzoic acid by replacing hydroxyl group sites on CNFs. Notably, the addition of CNFs into wheat gluten influenced the FTIR spectra and confirmed the presence of amide bands along with NFs, while the hydrophobic modification significantly reduced solubility. Furthermore, the introduction of antimicrobial properties through chitosan and salicylic acid contributed to the overall versatility of these biocomposite, positioning them as promising alternative to conventional synthetic materials in various applications. The ongoing exploration of diverse surface modifications holds promise for tailoring cellulose nanofibers to specific applications, optimizing their performance in various environments. Additionally, the synergistic combination of cellulose and wheat gluten inspired the development of novel biocomposite materials with enhanced mechanical, thermal, and barrier properties, which can be used for different potential applications including food packaging, biodegradable plastics, biomedical materials, automotive components, agricultural films, and in electronic devices due to their electroconductive nature. Further research may delve into scaling up production processes for these sustainable materials, paving the way for large-scale industrial applications.

CHAPTER 5

References

1. Nagarajan, K., et al., *Preparation of bio-eco based cellulose nanomaterials from used disposal paper cups through citric acid hydrolysis.* Carbohydrate polymers, 2020. **235**: p. 115997.
2. Li, T., et al., *Developing fibrillated cellulose as a sustainable technological material.* Nature, 2021. **590**(7844): p. 47-56.
3. Azizi Samir, M.A.S., F. Alloin, and A. Dufresne, *Review of recent research into cellulosic whiskers, their properties and their application in nanocomposite field.* Biomacromolecules, 2005. **6**(2): p. 612-626.
4. Liang, H.W., et al., *Robust and highly efficient free-standing carbonaceous nanofiber membranes for water purification.* Advanced Functional Materials, 2011. **21**(20): p. 3851-3858.
5. Nakagaito, A.N. and H. Yano, *Novel high-strength biocomposites based on microfibrillated cellulose having nano-order-unit web-like network structure.* Applied Physics A, 2005. **80**: p. 155-159.
6. Tonoli, G., et al., *Cellulose micro/nanofibres from Eucalyptus kraft pulp: preparation and properties.* Carbohydrate polymers, 2012. **89**(1): p. 80-88.
7. Kaur, M., P. Sharma, and S. Kumari, *State of art manufacturing and producing nanocellulose from agricultural waste: a review.* Journal of Nanoscience and Nanotechnology, 2021. **21**(6): p. 3394-3403.
8. Boswell, J., *The biological decomposition of cellulose.* The New Phytologist, 1941. **40**(1): p. 20-33.
9. Asyraf, M., et al., *Dynamic mechanical behaviour of kenaf cellulosic fibre biocomposites: A comprehensive review on chemical treatments.* Cellulose, 2021. **28**: p. 2675-2695.
10. Pandey, A., *Pharmaceutical and biomedical applications of cellulose nanofibers: a review.* Environmental Chemistry Letters, 2021. **19**(3): p. 2043-2055.
11. Poyraz, B., et al., *TEMPO-treated CNF composites: pulp and matrix effect.* Fibers and Polymers, 2018. **19**: p. 195-204.

12. Alves, L., et al., *Tuning rheology and aggregation behaviour of TEMPO-oxidised cellulose nanofibrils aqueous suspensions by addition of different acids.* Carbohydrate polymers, 2020. **237**: p. 116109.
13. Jonasson, S., et al., *Isolation and characterization of cellulose nanofibers from aspen wood using derivatizing and non-derivatizing pretreatments.* Cellulose, 2020. **27**: p. 185-203.
14. Barbash, V., O. Yaschenko, and O. Shniruk, *Preparation and properties of nanocellulose from organosolv straw pulp.* Nanoscale Research Letters, 2017. **12**: p. 1-8.
15. Rol, F., et al., *Recent advances in surface-modified cellulose nanofibrils.* Progress in Polymer Science, 2019. **88**: p. 241-264.
16. Bendaoud, A., et al., *Nanostructured cellulose-xyloglucan blends via ionic liquid/water processing.* Carbohydrate polymers, 2017. **168**: p. 163-172.
17. Qi, H., et al. *Homogenous carboxymethylation of cellulose in the new alkaline solvent LiOH/urea aqueous solution*. in *Macromolecular symposia*. 2010. Wiley Online Library.
18. Shaghaleh, H., X. Xu, and S. Wang, *Current progress in production of biopolymeric materials based on cellulose, cellulose nanofibers, and cellulose derivatives.* RSC advances, 2018. **8**(2): p. 825-842.
19. Xiao, H., M. Wu, and G. Zhao, *Electrocatalytic oxidation of cellulose to gluconate on carbon aerogel supported gold nanoparticles anode in alkaline medium.* Catalysts, 2015. **6**(1): p. 5.
20. Wang, W., et al., *Controlled graft polymerization on the surface of filter paper via enzyme-initiated RAFT polymerization.* Carbohydrate polymers, 2019. **207**: p. 239-245.
21. Yang, X., et al., *UV grafting: surface modification of cellulose nanofibers without the use of organic solvents.* Green Chemistry, 2019. **21**(17): p. 4619-4624.
22. Ramírez, J.A.Á., et al., *Surface esterification of cellulose nanofibers by a simple organocatalytic methodology.* Carbohydrate polymers, 2014. **114**: p. 416-423.
23. Sassi, J.-F. and H. Chanzy, *Ultrastructural aspects of the acetylation of cellulose.* Cellulose, 1995. **2**: p. 111-127.
24. Berlioz, S., et al., *Gas-phase surface esterification of cellulose microfibrils and whiskers.* Biomacromolecules, 2009. **10**(8): p. 2144-2151.
25. Singh, M., A. Kaushik, and D. Ahuja, *Surface functionalization of nanofibrillated cellulose extracted from wheat straw: Effect of process parameters.* Carbohydrate polymers, 2016. **150**: p. 48-56.
26. Vasconcelos, N.F., et al., *Chemically modified cellulose nanocrystals as polyanion for preparation of polyelectrolyte complex.* Cellulose, 2019. **26**: p. 1725-1746.

27. Türe, H., M. Gällstedt, and M.S. Hedenqvist, *Antimicrobial compression-moulded wheat gluten films containing potassium sorbate.* Food Research International, 2012. **45**(1): p. 109-115.
28. Irissin-Mangata, J., et al., *New plasticizers for wheat gluten films.* European polymer journal, 2001. **37**(8): p. 1533-1541.
29. Jansens, K.J., et al., *Effect of molding conditions and moisture content on the mechanical properties of compression molded glassy, wheat gluten bioplastics.* Industrial Crops and Products, 2013. **44**: p. 480-487.
30. Lagrain, B., et al., *Molecular basis of processing wheat gluten toward biobased materials.* Biomacromolecules, 2010. **11**(3): p. 533-541.
31. Abdulkhani, A., et al., *Preparation and characterization of modified cellulose nanofibers reinforced polylactic acid nanocomposite.* Polymer testing, 2014. **35**: p. 73-79.
32. Chen, Y., et al., *Length-controlled cellulose nanofibrils produced using enzyme pretreatment and grinding.* Cellulose, 2017. **24**: p. 5431-5442.
33. Bagheri, V., et al., *The optimization of physico-mechanical properties of bionanocomposite films based on gluten/carboxymethyl cellulose/cellulose nanofiber using response surface methodology.* Polymer Testing, 2019. **78**: p. 105989.
34. Pose, S., et al., *The nanostructural characterization of strawberry pectins in pectate lyase or polygalacturonase silenced fruits elucidates their role in softening.* Carbohydrate Polymers, 2015. **132**: p. 134-145.
35. Moon, R.J., et al., *Cellulose nanomaterials review: structure, properties and nanocomposites.* Chemical Society Reviews, 2011. **40**(7): p. 3941-3994.
36. Trache, D., et al., *Recent progress in cellulose nanocrystals: sources and production.* Nanoscale, 2017. **9**(5): p. 1763-1786.
37. Jonoobi, M., et al., *Chemical composition, crystallinity and thermal degradation of bleached and unbleached kenaf bast (Hibiscus cannabinus) pulp and nanofiber.* BioResources, 2009. **4**(2): p. 626-639.
38. Brinchi, L., et al., *Production of nanocrystalline cellulose from lignocellulosic biomass: technology and applications.* Carbohydrate polymers, 2013. **94**(1): p. 154-169.
39. Gopakumar, D.A., et al., *Nanocellulose based aerogels for varying engineering applications.* Encyclopedia of renewable and sustainable materials, 2020. **2**: p. p. 155-165.
40. Onyianta, A.J., M. Dorris, and R.L. Williams, *Aqueous morpholine pre-treatment in cellulose nanofibril (CNF) production: comparison with carboxymethylation and TEMPO oxidisation pre-treatment methods.* Cellulose, 2018. **25**: p. 1047-1064.

41. Naderi, A., T. Lindström, and J. Sundström, *Carboxymethylated nanofibrillated cellulose: rheological studies.* Cellulose, 2014. **21**: p. 1561-1571.
42. Liimatainen, H., et al., *Sulfonated cellulose nanofibrils obtained from wood pulp through regioselective oxidative bisulfite pre-treatment.* Cellulose, 2013. **20**: p. 741-749.
43. Olszewska, A., et al., *The behaviour of cationic nanofibrillar cellulose in aqueous media.* Cellulose, 2011. **18**: p. 1213-1226.
44. Sirvio, J.A., M. Visanko, and H. Liimatainen, *Acidic deep eutectic solvents as hydrolytic media for cellulose nanocrystal production.* Biomacromolecules, 2016. **17**(9): p. 3025-3032.
45. Chen, Y.W., et al., *Production of new cellulose nanomaterial from red algae marine biomass Gelidium elegans.* Carbohydrate polymers, 2016. **151**: p. 1210-1219.
46. Alemdar, A. and M. Sain, *Biocomposites from wheat straw nanofibers: Morphology, thermal and mechanical properties.* Composites Science and Technology, 2008. **68**(2): p. 557-565.
47. Yarbrough, J.M., et al., *Multifunctional cellulolytic enzymes outperform processive fungal cellulases for coproduction of nanocellulose and biofuels.* Acs Nano, 2017. **11**(3): p. 3101-3109.
48. Vickers, N.J., *Animal communication: when i'm calling you, will you answer too?* Current biology, 2017. **27**(14): p. R713-R715.
49. Khalil, H.A., et al., *A review on nanocellulosic fibres as new material for sustainable packaging: Process and applications.* Renewable and Sustainable Energy Reviews, 2016. **64**: p. 823-836.
50. Turbak, A.F., F.W. Snyder, and K.R. Sandberg. *Microfibrillated cellulose, a new cellulose product: properties, uses, and commercial potential*. in *J Appl Polym Sci Appl Polym Symp*. 1983.
51. Kalia, S., et al., *Nanofibrillated cellulose: surface modification and potential applications.* Colloid and Polymer Science, 2014. **292**: p. 5-31.
52. Zimmermann, T., E. Pöhler, and T. Geiger, *Cellulose fibrils for polymer reinforcement.* Advanced engineering materials, 2004. **6**(9): p. 754-761.
53. Osong, S.H., S. Norgren, and P. Engstrand, *Processing of wood-based microfibrillated cellulose and nanofibrillated cellulose, and applications relating to papermaking: a review.* Cellulose, 2016. **23**: p. 93-123.
54. Siró, I. and D. Plackett, *Microfibrillated cellulose and new nanocomposite materials: a review.* Cellulose, 2010. **17**: p. 459-494.
55. Ho, T.T.T., et al., *Nanofibrillation of pulp fibers by twin-screw extrusion.* Cellulose, 2015. **22**: p. 421-433.

56. Dufresne, A., *Nanocellulose: a new ageless bionanomaterial.* Materials today, 2013. **16**(6): p. 220-227.
57. Uetani, K. and H. Yano, *Nanofibrillation of wood pulp using a high-speed blender.* Biomacromolecules, 2011. **12**(2): p. 348-353.
58. Lavoine, N., et al., *Microfibrillated cellulose–Its barrier properties and applications in cellulosic materials: A review.* Carbohydrate polymers, 2012. **90**(2): p. 735-764.
59. Pedersen, A.L., et al., *DSM criteria that best differentiate intellectual disability from autism spectrum disorder.* Child Psychiatry & Human Development, 2017. **48**: p. 537-545.
60. George, J. and S. Sabapathi, *Cellulose nanocrystals: synthesis, functional properties, and applications.* Nanotechnology, science and applications, 2015: p. 45-54.
61. Shayestehkia, M., et al., *Effects of cellulose nanocrystals as extender on physical and mechanical properties of wood cement composite panels.* BioResources, 2020. **15**(4): p. 8291.
62. Aziz, T., et al., *Enhancement in adhesive and thermal properties of bio-based epoxy resin by using eugenol grafted cellulose nanocrystals.* Journal of Inorganic and Organometallic Polymers and Materials, 2021. **31**: p. 3290-3300.
63. Aziz, T., et al., *Manufactures of bio-degradable and bio-based polymers for bio-materials in the pharmaceutical field.* Journal of Applied Polymer Science, 2022. **139**(29): p. e52624.
64. Aziz, T., et al., *A Review on the Modification of Cellulose and Its Applications. Polymers 2022, 14, 3206*. 2022, s Note: MDPI stays neu-tral with regard to jurisdictional claims in ….
65. Culica, M.E., et al., *Cellulose surface modification for improved attachment of carbon nanotubes.* Cellulose, 2022. **29**(11): p. 6057-6076.
66. Isogai, A., *TEMPO-catalyzed oxidation of polysaccharides.* Polymer Journal, 2022. **54**(4): p. 387-402.
67. Akhlaghi, S.P., et al., *Synthesis of amine functionalized cellulose nanocrystals: optimization and characterization.* Carbohydrate research, 2015. **409**: p. 48-55.
68. Selim, A., et al., *Thiol-Functionalized Cellulose Wrapped Copperoxide as a Green Nano Catalyst for Regiospecific Azide-Alkyne Cycloaddition Reaction: Application in Rufinamide Synthesis.* Asian Journal of Organic Chemistry, 2021. **10**(12): p. 3428-3433.
69. Bahsis, L., et al., *Cellulose-copper as bio-supported recyclable catalyst for the clickable azide-alkyne [3+ 2] cycloaddition reaction in water.* International journal of biological macromolecules, 2018. **119**: p. 849-856.
70. Goldmann, A.S., et al., *Mild and Modular Surface Modification of Cellulose via Hetero Diels–Alder (HDA) Cycloaddition.* Biomacromolecules, 2011. **12**(4): p. 1137-1145.

71. Andrea, H., et al., *Temperature Responsive Cellulose-graft-Copolymers via Cellulose Functionalization in an Ionic Liquid and RAFT Polymerization.* 2014.
72. Ding, Q., et al., *New insights into the autofluorescence properties of cellulose/nanocellulose.* Scientific reports, 2020. **10**(1): p. 21387.
73. Beyler Çiğil, A., et al., *Cellulose/cysteine based thiol-ene UV cured adsorbent: removal of silver (I) ions from aqueous solution.* Cellulose, 2021. **28**(10): p. 6439-6448.
74. Yang, Q., et al., *Synthesis and characterization of cellulose fibers grafted with hyperbranched poly (3-methyl-3-oxetanemethanol).* Cellulose, 2011. **18**: p. 1611-1621.
75. Nguyen, D.T. and Q.T. Pham, *A theoretical and experimental study on etherification of primary alcohols with the hydroxyl groups of cellulose chain (n= 1–3) in acidic condition.* Journal of Molecular Structure, 2021. **1236**: p. 130314.
76. Fox, S.C., et al., *Regioselective esterification and etherification of cellulose: a review.* Biomacromolecules, 2011. **12**(6): p. 1956-1972.
77. Alven, S. and B.A. Aderibigbe, *Chitosan and cellulose-based hydrogels for wound management.* International journal of molecular sciences, 2020. **21**(24): p. 9656.
78. Srirachya, N., K. Boonkerd, and T. Kobayashi, *Effective elongation properties of cellulose–natural rubber composite hydrogels having interconnected domain.* Journal of Elastomers & Plastics, 2020. **52**(4): p. 337-355.
79. Sannino, A., et al., *Cellulose-based hydrogels as body water retainers.* Journal of materials science: materials in medicine, 2000. **11**: p. 247-253.
80. Zhang, Y.J., et al., *Cellulose tris (3, 5-dimethylphenylcarbamate) regioselectively bonded to small pore silica gel as chiral stationary phase for HPLC.* Applied Mechanics and Materials, 2012. **117**: p. 1361-1364.
81. Aloulou, F., S. Boufi, and J. Labidi, *Modified cellulose fibres for adsorption of organic compound in aqueous solution.* Separation and Purification Technology, 2006. **52**(2): p. 332-342.
82. Missoum, K., M.N. Belgacem, and J. Bras, *Nanofibrillated cellulose surface modification: a review.* Materials, 2013. **6**(5): p. 1745-1766.
83. Chhajed, M., et al., *Esterified superhydrophobic nanofibrillated cellulose based aerogel for oil spill treatment.* Carbohydrate polymers, 2019. **226**: p. 115286.
84. Sehaqui, H., et al., *Highly carboxylated cellulose nanofibers via succinic anhydride esterification of wheat fibers and facile mechanical disintegration.* Biomacromolecules, 2017. **18**(1): p. 242-248.

85. Her, K., et al., *Esterification of cellulose nanofibers with valeric acid and hexanoic acid.* Macromolecular Research, 2020. **28**: p. 1055-1063.
86. Baraka, F., E. Robles, and J. Labidi, *Microwave-assisted esterification of bleached and unbleached cellulose nanofibers.* Industrial Crops and Products, 2023. **191**: p. 115970.
87. Satgé, C., et al., *Rapid homogeneous esterification of cellulose induced by microwave irradiation.* Carbohydrate Polymers, 2002. **49**(3): p. 373-376.
88. Semsarilar, M. and S. Perrier, *Solubilization and functionalization of cellulose assisted by microwave irradiation.* Australian journal of chemistry, 2009. **62**(3): p. 223-226.
89. Rasheed, F., *Tailoring the structure-function relationship in wheat gluten.* Acta Universitatis Agriculturae Sueciae, 2015(2015: 13).
90. Tibolla, H., et al., *Starch-based nanocomposites with cellulose nanofibers obtained from chemical and mechanical treatments.* International journal of biological macromolecules, 2020. **161**: p. 132-146.
91. Follain, N., et al., *Water transport properties of bio-nanocomposites reinforced by Luffa cylindrica cellulose nanocrystals.* Journal of membrane science, 2013. **427**: p. 218-229.
92. MacRitchie, F., *Physicochemical properties of wheat proteins in relation to functionality*, in *Advances in food and nutrition research*. 1992, Elsevier. p. 1-87.
93. Domenek, S., et al., *Biodegradability of wheat gluten based bioplastics.* Chemosphere, 2004. **54**(4): p. 551-559.
94. Pouplin, M., A. Redl, and N. Gontard, *Glass transition of wheat gluten plasticized with water, glycerol, or sorbitol.* Journal of agricultural and food chemistry, 1999. **47**(2): p. 538-543.
95. Pommet, M., et al., *Study of wheat gluten plasticization with fatty acids.* Polymer, 2003. **44**(1): p. 115-122.
96. Pommet, M., et al., *Intrinsic influence of various plasticizers on functional properties and reactivity of wheat gluten thermoplastic materials.* Journal of cereal science, 2005. **42**(1): p. 81-91.
97. Pommet, M., et al., *Aggregation and degradation of plasticized wheat gluten during thermo-mechanical treatments, as monitored by rheological and biochemical changes.* Polymer, 2004. **45**(20): p. 6853-6860.
98. Woerdeman, D.L., et al., *Designing new materials from wheat protein.* Biomacromolecules, 2004. **5**(4): p. 1262-1269.
99. Zhang, J., P. Mungara, and J.-l. Jane, *Mechanical and thermal properties of extruded soy protein sheets.* Polymer, 2001. **42**(6): p. 2569-2578.

100. Zhang, X., et al., *pH effect on the mechanical performance and phase mobility of thermally processed wheat gluten-based natural polymer materials.* Biomacromolecules, 2006. **7**(12): p. 3466-3473.

101. Kunanopparat, T., et al., *Reinforcement of plasticized wheat gluten with natural fibers: from mechanical improvement to deplasticizing effect.* Composites part A: Applied science and manufacturing, 2008. **39**(5): p. 777-785.

102. Wretfors, C., et al., *Use of industrial hemp fibers to reinforce wheat gluten plastics.* Journal of Polymers and the Environment, 2009. **17**: p. 259-266.

103. Rudin, A. and P. Choi, *The elements of polymer science and engineering*. 2012: Academic press.

104. Sun, S., Y. Song, and Q. Zheng, *Thermo-molded wheat gluten plastics plasticized with glycerol: effect of molding temperature.* Food Hydrocolloids, 2008. **22**(6): p. 1006-1013.

105. Domenek, S., et al., *Polymerization kinetics of wheat gluten upon thermosetting. A mechanistic model.* Journal of Agricultural and Food Chemistry, 2002. **50**(21): p. 5947-5954.

106. Mungara, P., et al., *Processing and physical properties of plastics made from soy protein polyester blends.* Journal of Polymers and the Environment, 2002. **10**: p. 31-37.

107. John, J. and M. Bhattacharya, *Properties of reactively blended soy protein and modified polyesters.* Polymer international, 1999. **48**(11): p. 1165-1172.

108. Muensri, P., et al., *Effect of lignin removal on the properties of coconut coir fiber/wheat gluten biocomposite.* Composites Part A: Applied Science and Manufacturing, 2011. **42**(2): p. 173-179.

109. Liu, W., et al., *'Green'composites from soy based plastic and pineapple leaf fiber: fabrication and properties evaluation.* Polymer, 2005. **46**(8): p. 2710-2721.

110. Alizadeh-Sani, M., A. Khezerlou, and A. Ehsani, *Fabrication and characterization of the bionanocomposite film based on whey protein biopolymer loaded with TiO2 nanoparticles, cellulose nanofibers and rosemary essential oil.* Industrial crops and products, 2018. **124**: p. 300-315.

111. Fortunati, E., et al., *Revalorization of sunflower stalks as novel sources of cellulose nanofibrils and nanocrystals and their effect on wheat gluten bionanocomposite properties.* Carbohydrate polymers, 2016. **149**: p. 357-368.

112. Yang, W., et al., *Thermomechanical, antioxidant and moisture behaviour of PVA films in presence of citric acid esterified cellulose nanocrystals.* International Journal of Biological Macromolecules, 2020. **161**: p. 617-626.

113. Gadhave, R.V., C.R. Gadhave, and P.V. Dhawale, *Plastic-free bioactive paper coatings, way to next-generation sustainable paper packaging application: A review.* Green and Sustainable Chemistry, 2022. **12**(2): p. 9-27.
114. Saba, N. and M. Jawaid, *Recent advances in nanocellulose-based polymer nanocomposites.* Cellulose-Reinforced Nanofibre Composites, 2017: p. 89-112.
115. Freemantle, M., *An introduction to ionic liquids*. 2010: Royal Society of chemistry.
116. Nakashima, K., et al., *Feasibility of ionic liquids as alternative separation media for industrial solvent extraction processes.* Industrial & Engineering Chemistry Research, 2005. **44**(12): p. 4368-4372.
117. Shamshina, J.L., P.S. Barber, and R.D. Rogers, *Ionic liquids in drug delivery.* Expert opinion on drug delivery, 2013. **10**(10): p. 1367-1381.
118. Zajac, A., et al., *Ionic liquids as bioactive chemical tools for use in agriculture and the preservation of agricultural products.* Green Chemistry, 2018. **20**(21): p. 4764-4789.
119. Marullo, S., et al., *Ionic liquids gels: Soft materials for environmental remediation.* Journal of colloid and interface science, 2018. **517**: p. 182-193.
120. Bermúdez, M.-D., et al., *Ionic liquids as advanced lubricant fluids.* Molecules, 2009. **14**(8): p. 2888-2908.
121. Gu, Y. and G. Li, *Ionic liquids-based catalysis with solids: state of the art.* Advanced Synthesis & Catalysis, 2009. **351**(6): p. 817-847.
122. Potdar, M.K., et al., *Recent developments in chemical synthesis with biocatalysts in ionic liquids.* Molecules, 2015. **20**(9): p. 16788-16816.
123. Isik, M., H. Sardon, and D. Mecerreyes, *Ionic liquids and cellulose: dissolution, chemical modification and preparation of new cellulosic materials.* International journal of molecular sciences, 2014. **15**(7): p. 11922-11940.
124. RP, S., *Dissolution of cellulose with ionic liquids.* J Am Chem Soc, 2002. **124**: p. 4947-4975.
125. Gericke, M., P. Fardim, and T. Heinze, *Ionic liquids—promising but challenging solvents for homogeneous derivatization of cellulose.* Molecules, 2012. **17**(6): p. 7458-7502.
126. Kadokawa, J.-i., et al., *Preparation of cellulose–starch composite gel and fibrous material from a mixture of the polysaccharides in ionic liquid.* Carbohydrate Polymers, 2009. **75**(1): p. 180-183.
127. Murakami, M.-a., Y. Kaneko, and J.-i. Kadokawa, *Preparation of cellulose-polymerized ionic liquid composite by in-situ polymerization of polymerizable ionic liquid in cellulose-dissolving solution.* Carbohydrate polymers, 2007. **69**(2): p. 378-381.

128. Kumar, R., et al., *A simple approach for the isolation of cellulose nanofibers from banana fibers.* Materials Research Express, 2019. **6**(10): p. 105601.

129. Fatahi, S., et al., *The effects of chitosan supplementation on anthropometric indicators of obesity, lipid and glycemic profiles, and appetite-regulated hormones in adolescents with overweight or obesity: A randomized, double-blind clinical trial.* BMC pediatrics, 2022. **22**(1): p. 527.

130. *KGaA, M., IR Spectrum Table & Chart. 2021.*

131. Panchal, P. and T.H. Mekonnen, *Tailored cellulose nanocrystals as a functional ultraviolet absorbing nanofiller of epoxy polymers.* Nanoscale Advances, 2019. **1**(7): p. 2612-2623.

132. Kristianingrum, S., *Spektroskopi ultra violet dan sinar tampak (spektroskopi Uv-Vis).* Yogyakarta: Universitas Negeri Yogyakarta, 2016.

133. Mohammadi, M., A. Zoghi, and M.H. Azizi, *Assessment of properties of gluten-based edible film formulated with beeswax and DATEM for hamburger bread coating.* Food Science & Nutrition, 2023. **11**(4): p. 2061-2068.

134. Castro, G.R.d., et al., *Synthesis, characterization and determination of the metal ions adsorption capacity of cellulose modified with p-aminobenzoic groups.* Materials Research, 2004. **7**: p. 329-334.

135. Zuluaga, R., et al., *Cellulose microfibrils from banana rachis: Effect of alkaline treatments on structural and morphological features.* Carbohydrate Polymers, 2009. **76**(1): p. 51-59.

136. Pelissari, F.M., P.J.d.A. Sobral, and F.C. Menegalli, *Isolation and characterization of cellulose nanofibers from banana peels.* Cellulose, 2014. **21**: p. 417-432.

137. Li, Y., et al., *Facile extraction of cellulose nanocrystals from wood using ethanol and peroxide solvothermal pretreatment followed by ultrasonic nanofibrillation.* Green Chemistry, 2016. **18**(4): p. 1010-1018.

138. Li, W., et al., *Polymer conformation structure of wheat proteins and gluten subfractions revealed by ATR-FTIR.* Cereal Chemistry, 2006. **83**(4): p. 407-410.

139. Georget, D.M. and P.S. Belton, *Effects of temperature and water content on the secondary structure of wheat gluten studied by FTIR spectroscopy.* Biomacromolecules, 2006. **7**(2): p. 469-475.

140. Fang, Y., et al., *Mechanical properties and antibacterial activities of novel starch-based composite films incorporated with salicylic acid.* International journal of biological macromolecules, 2020. **155**: p. 1350-1358.